

AD-A031 766

BATTELLE COLUMBUS LABS OHIO
HIGH TEMPERATURE CREEP OF CERAMICS.(U)
JUN 76 M S SELTZER

F/G 11/2

UNCLASSIFIED

AFML-TR-76-97

F33615-73-C-4111
NL

1 OF 1
ADA031766



END

DATE
FILMED

12 -76

ADA031766

AFML-TR-76-97

fl. 712

HIGH TEMPERATURE CREEP OF CERAMICS

BATTELLE
COLUMBUS LABORATORIES
505 KING AVENUE
COLUMBUS, OHIO 43201

JUNE 1976

FINAL REPORT FOR PERIOD 1 FEBRUARY 1973 - 31 JANUARY 1976

Approved for public release; distribution unlimited

AIR FORCE MATERIALS LABORATORY
AIR FORCE WRIGHT AERONAUTICAL LABORATORIES
AIR FORCE SYSTEM COMMAND
WRIGHT-PATTERSON AIR FORCE BASE, OHIO 45433

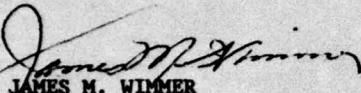


NOTICE

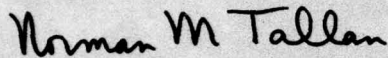
When Government drawings, specifications, or other data are used for any purpose other than in connection with a definitely related Government procurement operation, the United States Government thereby incurs no responsibility nor any obligation whatsoever; and the fact that the government may have formulated, furnished, or in any way supplied the said drawings, specifications, or other data, is not to be regarded by implication or otherwise as in any manner licensing the holder or any other person or corporation, or conveying any rights or permission to manufacture, use, or sell any patented invention that may in any way be related thereto.

This report has been reviewed by the Information Office (OI) and is releasable to the National Technical Information Service (NTIS). At NTIS, it will be available to the general public, including foreign nationals.

This technical report has been reviewed and is approved for publication.


JAMES M. WIMMER
Project Engineer

FOR THE COMMANDER


NORMAN M. TALLAN
Acting Chief, Processing and High
Temperature Materials Branch
Metals and Ceramics Division
Air Force Materials Laboratory

Copies of this report should not be returned unless return is required by security considerations, contractual obligations, or notice on a specific document.

SECURITY CLASSIFICATION OF THIS PAGE (When Data Entered)

REPORT DOCUMENTATION PAGE		READ INSTRUCTIONS BEFORE COMPLETING FORM
1. REPORT NUMBER AFML-TR-76-97	2. GOVT ACCESSION NO.	3. RECIPIENT'S CATALOG NUMBER
4. TITLE (and Subtitle) HIGH TEMPERATURE CREEP OF CERAMICS	5. TYPE OF REPORT & PERIOD COVERED Final 1 Feb 73 - 31 Jan 76	
7. AUTHOR(s) Martin S. Seltzer	8. CONTRACT OR GRANT NUMBER(s) F33615-73-C-4111	
9. PERFORMING ORGANIZATION NAME AND ADDRESS Battelle Columbus Laboratories 505 King Avenue Columbus, Ohio 43201	10. PROGRAM ELEMENT, PROJECT, TASK AREA & WORK UNIT NUMBERS 61102F, 7021, 702102 70210269	
11. CONTROLLING OFFICE NAME AND ADDRESS Air Force Materials Laboratory (LLM) Air Force Wright Aeronautical Laboratories Air Force Systems Command Wright-Patterson Air Force Base, Ohio 45422	12. REPORT DATE June 1976	
14. MONITORING AGENCY NAME & ADDRESS (if different from Controlling Office)	13. NUMBER OF PAGES 61	
	15. SECURITY CLASS. (of this report)	
15a. DECLASSIFICATION/DOWNGRADING SCHEDULE		
16. DISTRIBUTION STATEMENT (of this Report) Approved for public release; distribution unlimited.		
17. DISTRIBUTION STATEMENT (of the abstract entered in Block 20, if different from Report)		
18. SUPPLEMENTARY NOTES		
19. KEY WORDS (Continue on reverse side if necessary and identify by block number) Creep Silicon nitride ZrO ₂ Zirconia Sialon Si ₃ N ₄ Ceramics Stabilized zirconia		
20. ABSTRACT (Continue on reverse side if necessary and identify by block number) Tensile and compression creep measurements were made on yttria-stabilized zirconia (YSZ), hot-pressed silicon nitride and silicon materials, in atmospheres including air, nitrogen, argon and vacuum. For relatively fine-grained YSZ (below 40 microns), the 1.5 power of the applied stress at low stresses and with the stress cubed at high stresses, but results for coarse grained specimens can generally be fitted by the cube dependence. Creep activation energies for YSZ are found to be 128 kcal/mole independent of yttria content, impurity level, grain size and porosity distribution. For the silicon compounds, at least two		

DD FORM 1 JAN 73 1473 EDITION OF 1 NOV 65 IS OBSOLETE

SECURITY CLASSIFICATION OF THIS PAGE (When Data Entered)

407 080

bpj

20. ABSTRACT (Continued)

different creep mechanisms are operative in the range of temperatures and stresses employed in this study. A grain boundary sliding mechanism, characterized by a stress dependence of two and an activation energy of 168 kcal/mole, appears to be operative for hot-pressed silicon nitride; but a viscous creep mechanism predominates for some SiAlON materials, where a linear stress dependence and an activation energy of 94 kcal/mole have been measured.

ACCESSION for		
NTIS	White Section	<input checked="" type="checkbox"/>
DOC	Buff Section	<input type="checkbox"/>
UNANNOUNCED		<input type="checkbox"/>
JUSTIFICATION.....		
BY.....		
DISTRIBUTION/AVAILABILITY CODES		
Dist.	AVAIL. and/or SPECIAL	
A		

FOREWORD

This is a final technical report prepared by the Metal Science Section of Battelle's Columbus Laboratories describing a study on the high temperature creep behavior of yttria stabilized zirconia and of silicon-base compounds. The research described in this report was conducted under Contract No. F33615-73-C-4111 from February 1, 1973 to January 31, 1976 at Battelle's Columbus Laboratories. Program monitors were Lt. Patrick K. Talty and Dr. James M. Wimmer of the Metallurgy and Ceramics Laboratory (LL), Aerospace Research Laboratories (AFSC), Wright-Patterson AFB, Ohio 45433. The work performed on this contract dealing with creep of yttria stabilized zirconia was reported in ARL TR 75-0023, "High Temperature Compressive Creep of Yttria Stabilized Zirconia" by P. K. Talty (ARL) and M. S. Seltzer, March, 1975.

Lawrence Coubrough (Coors Porcelain Company) and Karl Fuchs (Zircoa Division of Corhart Refractories Company) provided yttria-stabilized zirconia specimens. C. R. Tinsley (ARO, Inc.) provided yttria-stabilized zirconia brick from the pilot storage heater at the Arnold Engineering Development Center.

Specimens of silicon nitride were provided by Ronald K. Bart of the Norton Company, and SiALON materials were supplied by Dr. F. Lange of the Westinghouse Electric Corporation, Dr. J. M. Wimmer of ARL and Dr. T. Wright of Battelle's Columbus Laboratories.

The creep experiments were performed by J. R. Bibler, and most of the metallography was performed by C. R. Thompson and G. A. Wheeler.



TABLE OF CONTENTS

SECTION		PAGE
I	INTRODUCTION	1
II	BACKGROUND	4
III	EXPERIMENTAL PROCEDURES	9
	1. Specimen Preparation	9
	2. Creep Testing	11
	3. Materials Characterization	12
IV	EXPERIMENTAL RESULTS	14
	1. Material Characterization	14
	2. Creep of Silicon-Base Materials	24
V	DISCUSSION	51
VI	CONCLUSIONS	58
	REFERENCES	60

LIST OF ILLUSTRATIONS

FIGURE		PAGE
1	OPTICAL MICROGRAPHS OF POLISHED SECTIONS OF Si_3N_4 AND OF VARIOUS SiAlONs	15
2	OPTICAL MICROGRAPHS OF POLISHED SECTIONS OF Si_3N_4 AND OF VARIOUS SiAlONs	16
3	MICROSTRUCTURES OF POLISHED AND ETCHED LONGITUDINAL SECTIONS OF Si_3N_4 AND OF VARIOUS SiAlONs	17
4	MICROSTRUCTURES OF POLISHED AND ETCHED LONGITUDINAL SECTIONS OF Si_3N_4 AND OF VARIOUS SiAlONs	18
5	MICROSTRUCTURE OF ETCHED FRACTURE SURFACE OF G20A1ON AS-FABRICATED	20
6	SCANNING ELECTRON MICROGRAPHS OF Si_3N_4 AND OF VARIOUS SiAlONs	21
7	OPTICAL MICROGRAPHS OF POLISHED SECTIONS OF VARIOUS SiAlONs	22
8	MICROSTRUCTURES OF POLISHED AND ETCHED SECTIONS OF VARIOUS SiAlONs	23
9	MICROSTRUCTURES OF POLISHED SECTIONS OF NC203, NC350, AND NC435	25
10	MICROSTRUCTURES OF POLISHED AND ETCHED LONGITUDINAL SECTIONS OF NC203 AND NC435	26
11	COMPRESSION CREEP STRAIN VERSUS TIME FOR HS130-1 TESTED IN AIR AT 1400°C	27
12	COMPRESSION CREEP STRAIN VERSUS TIME FOR SiAlON 59D-1 TESTED IN AIR AT 1400°C	28
13	STEADY-STATE CREEP RATE VERSUS APPLIED STRESS FOR HS130 TESTED IN AIR, ARGON AND NITROGEN	29
14	STEADY-STATE CREEP RATE VERSUS APPLIED STRESS FOR NORTON HOT-PRESSED Si_3N_4 TESTED IN AIR	32
15	STEADY-STATE CREEP RATE VERSUS RECIPROCAL ABSOLUTE TEMPERATURE FOR HOT-PRESSED Si_3N_4	33
16	STEADY-STATE CREEP RATE VERSUS APPLIED STRESS FOR HS130	35

LIST OF ILLUSTRATIONS (Continued)

FIGURE		PAGE
17	STEADY-STATE CREEP RATE VERSUS APPLIED STRESS FOR SIALON 59D TESTED IN AIR	36
18	STEADY-STATE CREEP RATE VERSUS RECIPROCAL ABSOLUTE TEMPERATURE FOR SIALON 59D TESTED IN AIR	37
19	COMPARISON OF CREEP DATA OBTAINED AS A FUNCTION OF STRESS AT 1400°C IN AIR FOR HS130 AND THREE DIFFERENT SIALON MATERIALS	39
20	STEADY-STATE CREEP RATE VERSUS APPLIED STRESS FOR SIALON 59D AND 65C TESTED IN AIR, ARGON, AND VACUUM AT 1400°C	40
21	STEADY-STATE CREEP RATE VERSUS APPLIED STRESS FOR SIALON 65C	41
22	STEADY-STATE CREEP RATE VERSUS APPLIED STRESS FOR HOT PRESSED Si_3N_4 AND FOR VARIOUS SIALON COMPOSITIONS . .	43
23	STEADY-STATE CREEP RATE VERSUS APPLIED STRESS FOR SIALON CONTAINING 40 AND 50 W/O Al_2O_3	46
24	STEADY-STATE CREEP RATE VERSUS APPLIED STRESS FOR SIALON CONTAINING 30 W/O Al_2O_3	47
25	COMPARISON OF CREEP DATA OBTAINED AS A FUNCTION OF STRESS AT 1400°C AND 1475°C IN AIR FOR HOT-PRESSED Si_3N_4 , REACTION-BONDED Si_3N_4 AND SIALON G20A1ON . . .	48
26	FOIL OF NC-132 ILLUSTRATING OPAQUE PARTICLES, DISLO- CATION ARRAYS WITHIN GRAINS, AND APPARENT STACKING FAULT CONTRAST	52
27	DISLOCATION ARRAYS	52

SECTION I

INTRODUCTION

The objective during the first year of this three-year program was to define the creep behavior of yttria-rare earth-stabilized zirconia (YRESZ) at very high temperatures (to 2000°C) under conditions of stress, temperature, and environment that are encountered in storage heaters used in "blow down" wind tunnels. Research at Battelle Columbus Laboratories (BCL), coupled with in-house creep studies at Aerospace Research Laboratories (ARL), was aimed at defining the influence of these variables on the creep strain and strain rate in order to predict the plastic deformation of the stabilized zirconia that will occur during operation of storage heaters. Initial studies were conducted on "standard" materials of the type which have been prepared for use in storage heaters by the Coors Porcelain Company and by the Zircoa Division of Corhart Refractories Company. In addition, studies were undertaken to examine the effect on creep behavior of: composition (YRE content), grain size, environment (air, inert gas, and vacuum), and "preexposure." Some of these investigations provided information which helped to define operative creep mechanisms. The "preexposure" creep experiments were conducted on specimens taken from storage heaters at the Arnold Engineering Development Center (AEDC) that had been in operation for various times. The purpose, here, was to determine whether or not the creep behavior of stabilized zirconia is affected by exposure to operating conditions in a storage heater. The results of these experiments were discussed in ARL TR 75-0023⁽¹⁾ and other publications⁽²⁾. The conclusions reached were as follows:

- (1) For a given grain size, creep rates for Coors and Zircoa high density YRESZ are nearly equal, in spite of differences in

impurity contents, pore size, and yttria/rare earth concentrations.

- (2) Massive grain boundary separation and lines of pores parallel to the stress axis are observed at strains above three percent for specimens tested below 1550°C, but no evidence for grain boundary sliding was observed for specimens tested at higher temperatures.
- (3) The activation energy for creep of YSZ above 1500°C is 128 ± 10 kcal/mole, independent of density, stress, and environment.
- (4) For as-fabricated high density YSZ with a grain size less than 40 μm creep rates are proportional to $\sigma^{1.5}$ at low stress levels. If the applied stresses are corrected for an apparent threshold stress, then creep rates are proportional to the effective stress.
- (5) For both high and low density specimens annealed above 1900°C, or those previously fired in the AEDC storage heater to 2240°C, a second stress dependence for which the stress exponent, n , is approximately 3 is observed. In some cases a deviation to lower stress exponents is found at low applied stresses. This phenomena is associated with the observation of substructure within grains of deformed samples.
- (6) Major microstructural modifications occur in low density YRESZ bricks by heating them to 2240°C in the AEDC storage heater. The grain size of high density bricks increases from 12-28 μm to about 75 μm , but the grain structure of low density bricks develop into a series of large grains with colonies of smaller grains, with no apparent increase in bulk density. The creep strength of fired low density YRESZ is more than an order of magnitude greater than

as-fabricated material tested at 1882°C after several days of equilibration at temperature.

- (7) Creep rates for YSZ increase with increasing oxygen partial pressure. Apparently the diffusion controlling process involves migration of neutral zirconium vacancies, or some other neutral species, whose concentration varies with oxygen pressure but is unaffected by aliovalent doping additions.
- (8) The creep strength for high density YSZ appears to be adequate for operation at 2250°C under stresses less than 50 psi. With proper annealing treatment, low density YRESZ can probably provide adequate creep resistance at storage-heater temperatures.

The major objective of the studies conducted in the second and third years of the program was to obtain a better understanding of the creep behavior of silicon nitride (Si_3N_4) and its alloys such as the SiAlON compounds. Studies were conducted over ranges of stress, temperature, and gaseous environment (e.g., nitrogen, argon, oxygen, and vacuum) on both tension and compression specimens to determine the creep mechanisms operative under various conditions and how environment might alter these mechanisms. The results of these studies have not been reported in the open literature, and will be presented in detail in this report.

SECTION II

BACKGROUND

After more than ten years of research at various laboratories, silicon nitride and its alloys have been established as materials with a number of potential high temperature engineering applications. Among the favorable properties of Si_3N_4 are a high melting point (dissociates at $\sim 1900^\circ\text{C}$ in 1 atm of nitrogen), a low coefficient of thermal expansion which leads to excellent thermal shock resistance, excellent oxidation resistance up to about 1400°C , and low density (3.19 g/cc for fully dense material). These properties, together with the advances in technology for preparation of silicon nitride shapes by reaction bonding and hot pressing, make this ceramic attractive for certain structural applications such as gas turbine components, high temperature bearings, high temperature radomes, and in combustion chamber structures.

Although the engineering design problems associated with the brittleness of any ceramic material under tensile stress must be solved before Si_3N_4 can be used to its envisioned potential, there also remain some materials considerations which must be examined in detail if this ceramic is to serve in high-temperature applications such as uncooled vanes of gas turbines. One of the most important properties which must be characterized and understood is the high-temperature creep behavior. Until recently only a few engineering-type creep tests had been conducted to examine the creep properties of silicon nitride.

Silicon nitride has been produced by a reaction-bonding process, which yields a low density (70-85% theoretical) material and by various hot pressing methods with different additives which give a high density ($> 99\%$ theoretical). The techniques for the preparation of these forms of Si_3N_4

are somewhat involved, and are described in great detail elsewhere⁽³⁻⁶⁾. Evans and Sharp⁽⁷⁾ have performed microstructural studies on typical samples of Si_3N_4 prepared by both methods. Briefly, the reaction-bonded material they examined was prepared by heating compacted silicon under nitrogen at two temperatures (two stage annealing), resulting in a structure which contained two hexagonal phases, α (60%) and β (40%), with a small amount ($\sim 2\%$) of unreacted silicon. Both pore size and grain size of this reaction-bonded Si_3N_4 varied over wide limits; from less than $1\ \mu\text{m}$ to greater than $25\ \mu\text{m}$ in diameter in both cases. Other investigators have shown that it is possible to vary the processing conditions to give different densities of reaction-bonded Si_3N_4 ⁽⁸⁾ and to vary the relative proportions of the α and β phases⁽⁹⁾.

The hot pressed Si_3N_4 that Evans and Sharp studied was prepared by J. Lucas, Ltd., using $\sim 5\%$ MgO additive, and consisted of 90% small angular $\beta\text{-Si}_3\text{N}_4$ grains and 10% $\alpha\text{-Si}_3\text{N}_4$. These specimens had small acicular grains varying in length from 0.1 to $2\ \mu\text{m}$ and some larger irregular grains up to $8\ \mu\text{m}$ in length. There was also some noncrystalline material between the angular grains along with numerous small unidentified inclusions.

Creep experiments have been performed on both kinds of Si_3N_4 . In an early study, Deeley, Herbert, and Moore⁽⁴⁾ reported that hot-pressed material prepared from 98% purity silicon had insufficient creep-resistance at 1200°C to be useful as a gas turbine blade material, but that satisfactory creep-strength could be achieved in Si_3N_4 prepared from 99.9% purity silicon. For some unknown reason, the use of purer silicon led to a reduction in thermal shock resistance. Quantitative results were not presented in this paper.

Glenny and Taylor⁽¹⁰⁾ investigated the four-point bending and, to a limited extent, tension creep characteristics of three types of reaction-bonded Si_3N_4 with typical bulk densities of 2.00-2.6 g/cm³, and one type of hot-pressed material which had densities in the range of 3.00-3.18 g/cm³. Bend tests were conducted (presumably in air) over the temperature range of 1000-1200°C at stresses of about 2200-58,000 psi. Specimens with less than 0.0235 in. midspan deflection (0.125% outer fiber tensile strain) after 100 hours under a bending stress of 4500 psi at temperatures above 1050°C were considered to be potentially useful for nozzle guide vanes.

The results of this study were complicated by possible changes in specimen structure and composition with temperature. For bend tests at 1200°C, however, it was found that reaction-bonded Si_3N_4 containing 5% silicon carbide exhibited excellent creep resistance (0.009 in. midspan deflection after 100 hours under 4500 psi). Dense, hot-pressed Si_3N_4 , derived from 98% purity silicon showed progressive deterioration in creep strength as temperature was increased from 1000 to 1200°C. At 1200°C a midspan deflection of 0.035 in. was measured after 25 hours under 4500 psi. Hot pressed material prepared from 99.9% purity silicon showed considerably superior creep strength at 1200°C, but the midspan deflection after 100 hours was still somewhat larger than was measured for the reaction-sintered material containing SiC. Tests were not performed on hot-pressed silicon nitride containing SiC additions.

Parr⁽¹¹⁾ performed bend-creep experiments on reaction-bonded silicon nitride at 1200°C, similar to those conducted by Glenny and Taylor. As in the previous study, 5% silicon carbide additions enhanced creep strength. In addition, Parr found that the midspan deflection was decreased by a factor of three when the specimen density was increased from 2.1 g/cc to 2.5 g/cc.

Preliminary four-point bend creep studies at 1200-1480°C on reaction-bonded Si_3N_4 by Thompson and Pratt⁽⁸⁾ showed that the creep strength of $\alpha\text{-Si}_3\text{N}_4$ decreased with increasing temperature and with increasing porosity, and that $\beta\text{-Si}_3\text{N}_4$ crept more rapidly than the α -phase.

Kossowsky⁽¹²⁾ has performed an extensive series of tensile and compressive creep tests on Norton HS130 containing various concentrations of alkaline earth impurities. He has shown that creep rates are a very sensitive function of calcium concentration, decreasing by some three orders of magnitude as the calcium level is decreased from 0.5 to 0.05 w/o. Creep rates obtained from tests conducted in air were about one-half order of magnitude greater than those obtained under a helium atmosphere. In addition, greater elongations were measured in tension tests performed in air (3-4%) as compared with tests performed in helium (0.2-0.6%) under stresses of 10,000-14,000 psi and temperatures in the range 1800-2500°F. The creep activation energies were about 130 kcal/mole for high purity HS130 tested in air and 150 kcal/mole for experiments performed in helium. Finally, the stress exponent, n , for steady-state creep was reported to have a value of about 2.

Based on these results and microstructural evidence, Kossowsky concluded that the data for HS130 are consistent with a grain boundary sliding mechanism. He suggested that a glassy magnesium silicate phase exists at the grain boundaries. The viscosity of this phase is believed to be greatly influenced by calcium, leading to a major reduction in creep strength with increasing calcium concentration.

The creep deformation of hot-pressed and reaction sintered silicon nitride has been also investigated by Ud Din and Nicholson.^(13,14) These authors used a four-point bending technique with stresses of 10,000-20,000 psi in the temperature range of 1200-1450°C to study the creep behavior of reaction-bonded Si_3N_4 prepared by slip-casting and injection molding. The creep activation energy was reported to be 130 ± 5 kcal/mole and the stress exponent was found to be 1.4. Microstructural evidence obtained from use of transmission and electron microscopy suggested that grain boundary sliding is the rate-controlling process for creep of this material. Similar tests performed on hot-pressed silicon nitride gave comparable values for n and Q_c to those reported for reaction-sintered material ($n = 1.7$ and $Q_c = 140$ kcal/mole). Creep behavior was again attributed to grain boundary sliding, accommodated by void deformation at triple points and by limited local plastic deformation.

Mangels et al.⁽¹⁵⁾ reported results for the creep behavior of reaction-sintered Si_3N_4 . They conducted four-point bend tests in air on material with 70-75% TD. Reducing the calcium concentration and performing the nitriding in a mixture of $\text{N}_2 + 1.8\%\text{H}_2$ rather than in pure N_2 , improved the creep strength. In these studies the stress exponent was found to be 1.6, and the creep activation energy was 50-55 kcal/mole.

Arrol⁽¹⁶⁾ has shown that the creep strength of hot-pressed SiAlON can be controlled over a wide range of values. The surface tensile strain for 100-hour tests conducted at 1225°C at a stress of 5 tsi was increased from 0.01% to greater than 0.3% with decreasing Al/Si ratio. For high Al/Si ratios (Specimen 121) creep strains were lower than those measured for the Lucas equivalent of Norton HS130 as well as reaction-bonded silicon nitride and hot-pressed silicon carbide.

SECTION III

EXPERIMENTAL PROCEDURES

1. Specimen Preparation

Tensile and compression creep samples were ultrasonically machined from large billets obtained from the Aerospace Research Laboratories, Battelle's Columbus Laboratories, Westinghouse Research Laboratories, and the Norton Company. The Norton material was HS130 and NC132 (two grades of high-density hot-pressed silicon nitride), NC350 which is a reaction bonded silicon nitride, NC203 which is hot-pressed SiC, and NC435 which is a fine-grained, densified SiC. SiAlON materials were obtained from ARL, Westinghouse and BCL. The SiAlON materials designated 59D, 65C, and SSI/R3 were prepared at ARL from 0.3 μm Linde A alumina and AME powdered Si_3N_4 with 6 and 7.5 w/o AlN and 2.5 w/o MgO. The ratio of Al/Si was the same as that for a 50:50 mole percent alloy of Al_2O_3 and Si_3N_4 . The 59D material was sintered at 1700°C for 24 hours in a nitrogen atmosphere, yielding a product with a density of 3.05 g/cm³. The 65C had a lower density, 2.71 g/cm³. The SSI/R3 material was isostatically pressed and sintered at 1750°C to a density of 3.02 g/cm³.

The SiAlON specimens designated G20AlON and G35AlON were prepared by T. Wright at Battelle-Columbus as described elsewhere.⁽¹⁷⁾ The Si_3N_4 powder used to prepare these specimens was obtained from Montecatini Edison. The starting material had 200 ppm of calcium and 1000 ppm of aluminum. The G20AlON material had an initial composition of 84.7 w/o Si_3N_4 , 0.34 w/o AlN and 14.95 w/o Al_2O_3 and a final composition corresponding to Si_3N_4 -20 mole percent Al_2O_3 . The bulk density was 3.15 g/cm³ with an average grain size of 1.02 μm . The initial composition of the G35AlON was 71.94 w/o Si_3N_4 ,

0.30 w/o AlN, and 27.76 w/o Al_2O_3 . After hot pressing at 1750°C for 1.5 hours under 5000 psi the material had a density of $\sim 98\%$ TD.

SiAlON specimens were also obtained from Dr. F. F. Lange of the Westinghouse Research Laboratories. These specimens, including compositions with 20, 30, 40 and 49.2 w/o Al_2O_3 , were prepared by hot-pressing at temperatures $\geq 1650^\circ\text{C}$. Thermal expansion and strength of these specimens, at room temperature and 1400°C , have been reported by Lange, along with fabrication parameters⁽¹⁸⁾. Major cation impurities in the starting Si_3N_4 powder, which was 90% α - Si_3N_4 -10% β - Si_3N_4 were 0.5 w/o Al, 0.5 w/o Fe, and 0.3 w/o Ca. It is also believed that the starting powder contained between 3 and 6 w/o SiO_2 . The high density SiAlON compositions contained between 2 and 3 w/o WC contaminate as a result of ball milling the Si_3N_4 - Al_2O_3 powders in a plastic bottle containing tungsten carbide ball mills prior to hot pressing.

Selected tests were also conducted on commercial grades of reaction-bonded silicon nitride (NC350), hot-pressed silicon carbide (NC203), and fine-grained densified silicon carbide (NC435) prepared by the Norton Company and obtained from the Aerospace Research Laboratories. The reaction-bonded silicon nitride with density in the range of 2.4-2.6 g/cc has a reported flexural strength of over 50000 psi at 1450°C , with no deformation or 4-point bending creep taking place under a load of 20000 psi at a temperature of 1260°C for 260 hrs.⁽¹⁹⁾ Hot-pressed silicon carbide (NC203) is reported to have slightly lower strength than NC132 at room temperature, but it appears to maintain its strength above 1300°C much better than does the NC132.⁽²⁰⁾ The fine-grained densified silicon carbide (NC435) has about half the room temperature flexural strength of NC203 but may have greater strength at temperatures above 1400°C .⁽²⁰⁾

2. Creep Testing

Creep studies have been performed under the following conditions:

(a) tension and compression, (b) temperatures in the range of 1220-1475°C, (c) stresses in the range of 1000 to 80,000 psi, (d) atmospheres including air, nitrogen, argon, and vacuum. Tension creep specimens had a "dogbone" configuration similar to those used previously on creep of MgO single crystals.⁽²¹⁾ They had a 1-inch gage length with a square gage cross section of 0.1 inch by 0.1 inch. Cylindrical compression creep specimens 0.34-inch long and 0.17 inch in diameter were used. This configuration is similar to that previously used for compression creep of YRESZ.

Tensile creep tests were performed in a high temperature vacuum furnace capable of reaching temperatures to 2000°C under 3×10^{-5} to 5×10^{-6} torr vacuum. The unit has a cylindrical tantalum heating element, surrounded by molybdenum radiation shields. Temperature is monitored by mounting a thermocouple bead in a small indentation in the side of the bottom grip. This ensures that the thermocouple is in exactly the same position each time.

Constant stress throughout the creep test was maintained with a contoured constant stress lever arm. The lever arm is mounted in a vacuum chamber attached to the creep furnace so that the entire loading system is enclosed with the vacuum. With this arrangement the load is transmitted to the specimen through knife edges, so that at low loads no errors are introduced through sliding seals or bearings. Creep strain is recorded continuously by means of a linear variable differential transformer system.

Compression creep tests were conducted in two different creep units. Tests in air or nitrogen were performed in an apparatus which utilizes molybdenum disilicide heating elements which permit operating

temperatures to 1600°C. The specimen chamber is an alumina tube, which allows creep experiments to be conducted in a variety of flowing gas mixtures. Strain over the specimen gage length alone is measured by determining the difference in deflection between silicon carbide disks placed above and below the specimen. Alumina push rods transmit the deflections to a linear variable differential transformer located below the loading frame. Deflections of 5×10^{-5} inch are measured and the strain is recorded continuously.

Compression creep tests in vacuum or in an argon atmosphere were performed in a tungsten-mesh constant-stress unit. Strain over the specimen gage length alone is measured by determining the difference in deflection between the tungsten platens above and below the specimen. Tungsten push rods transmit the deflection to a linear variable differential transducer located above the loading frame. Deflections of 5×10^{-5} inch are measured, and the strain is recorded continuously. Chart speeds from 1 in./sec to 0.1 in./hr permit detailed recording of instantaneous, primary and steady-state creep behavior. A sighting port allows direct observation of the specimen.

A constant-stress system ensured that the initial stress did not vary by more than 0.5 percent as the specimen was strained over several percent, without the necessity of adding load at regular intervals. Temperature was recorded continuously and controlled to at least $\pm 5^\circ\text{C}$ over the specimen gage length.

3. Materials Characterization

Careful characterization of the microstructures and composition of materials prior to and after creep under various conditions is a necessary step in any program aimed at understanding creep mechanisms.

This is particularly important for silicon-base compounds which have very heterogeneous microstructures and compositions. Characterization has been performed by utilization of

- (a) Optical metallography to reveal general microstructural features, e.g., unreacted elements or precipitates, distribution of porosity, grain size (if resolvable), creep-induced grain boundary sliding or wedge-type cracking.
- (b) Scanning and replica electron microscopy--on specimens fractured at room temperature, both before and after creep--to determine grain size, and distribution of porosity on grain boundaries.
- (c) Chemical analysis, including bulk spectrographic analysis for trace impurities.

SECTION IV

EXPERIMENTAL RESULTS

1. Material Characterization

Optical micrographs of as-polished surfaces of Si_3N_4 and of various SiAlONs are presented in Figures 1 and 2. Micrographs of HS130 and the SiAlON materials G20AlON, 59D, and 65C are presented in Figure 1. The HS130 is in the as-received condition while the three SiAlON micrographs were taken from longitudinal sections of specimens which had been subjected to compression creep at 1400°C . The phase distributions and pore structures are typical for these materials before or after creep. The HS130 and G20AlON appear to be almost fully dense while moderate and high-pore concentrations are found in the 59D and 65C. Several cracks are apparent in the SiAlON 65C (A and B in Figure 1d).

Figure 2 includes micrographs of as-polished surfaces of NC132, HS130, and the SiAlON materials SSI/R3 and G35AlON. The NC132 is in the as-received condition, while the other three micrographs were taken from longitudinal sections of specimens which had been subjected to compression creep at elevated temperature. The HS130 and NC132 appear to be almost fully dense while the two SiAlON materials have moderate pore concentrations (as compared with the SiAlON 65 C).

The grain structures obtained after etching (3-10 min in 20% NH_4FHF aqueous solution at 180°F) and replicating the surfaces shown in Figures 1 and 2 are presented in Figures 3 and 4. The SiAlON materials appear to have equiaxed coarse-grained structures as compared with the silicon nitride materials. The grain boundaries in the G20AlON are weakly

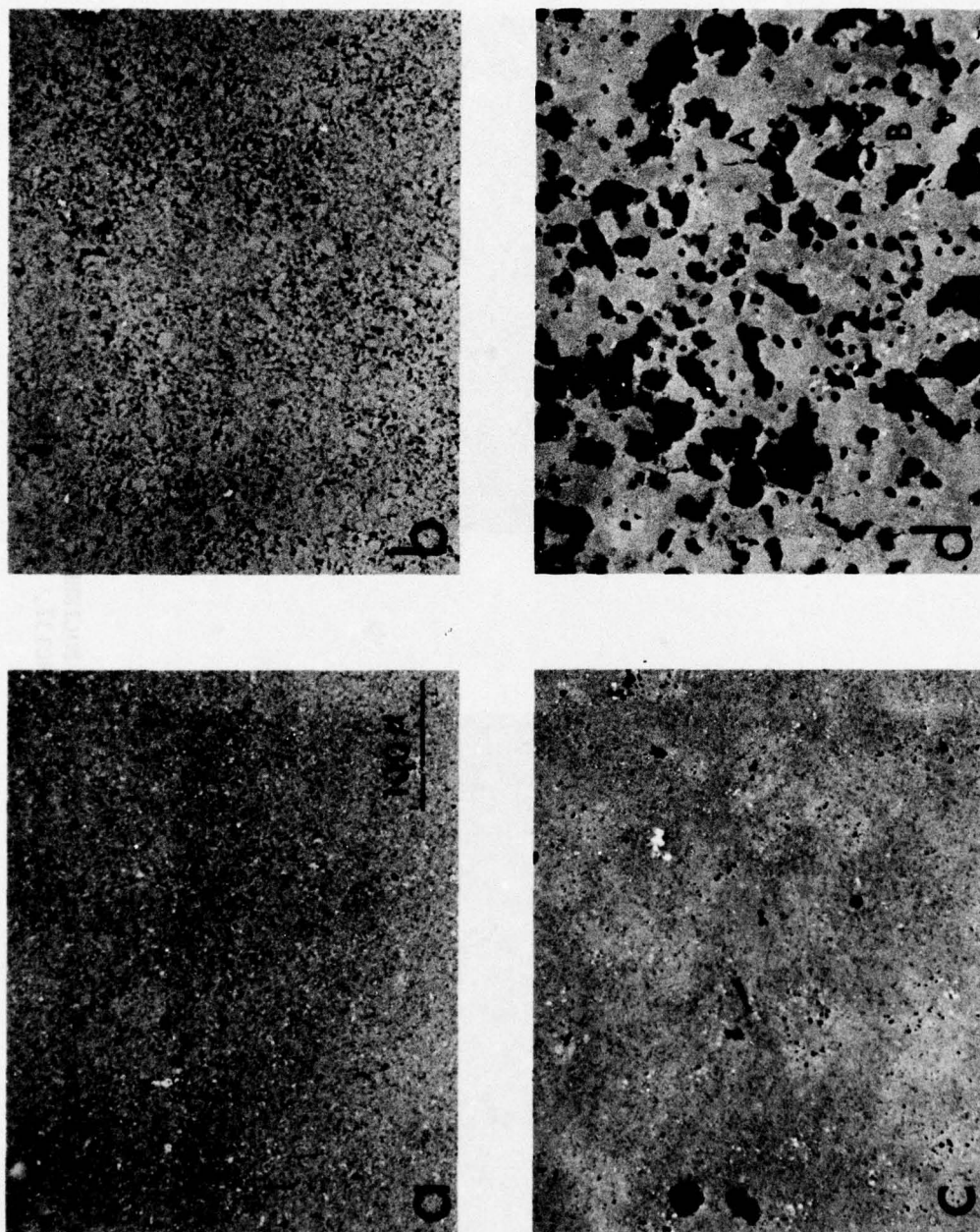


FIGURE 1. OPTICAL MICROGRAPHS OF POLISHED SECTIONS OF Si_3N_4 AND OF VARIOUS STIALONS:
 (a) HS130, (b) G20AION-1, (c) 59D-2, (d) 65C-1. 250X

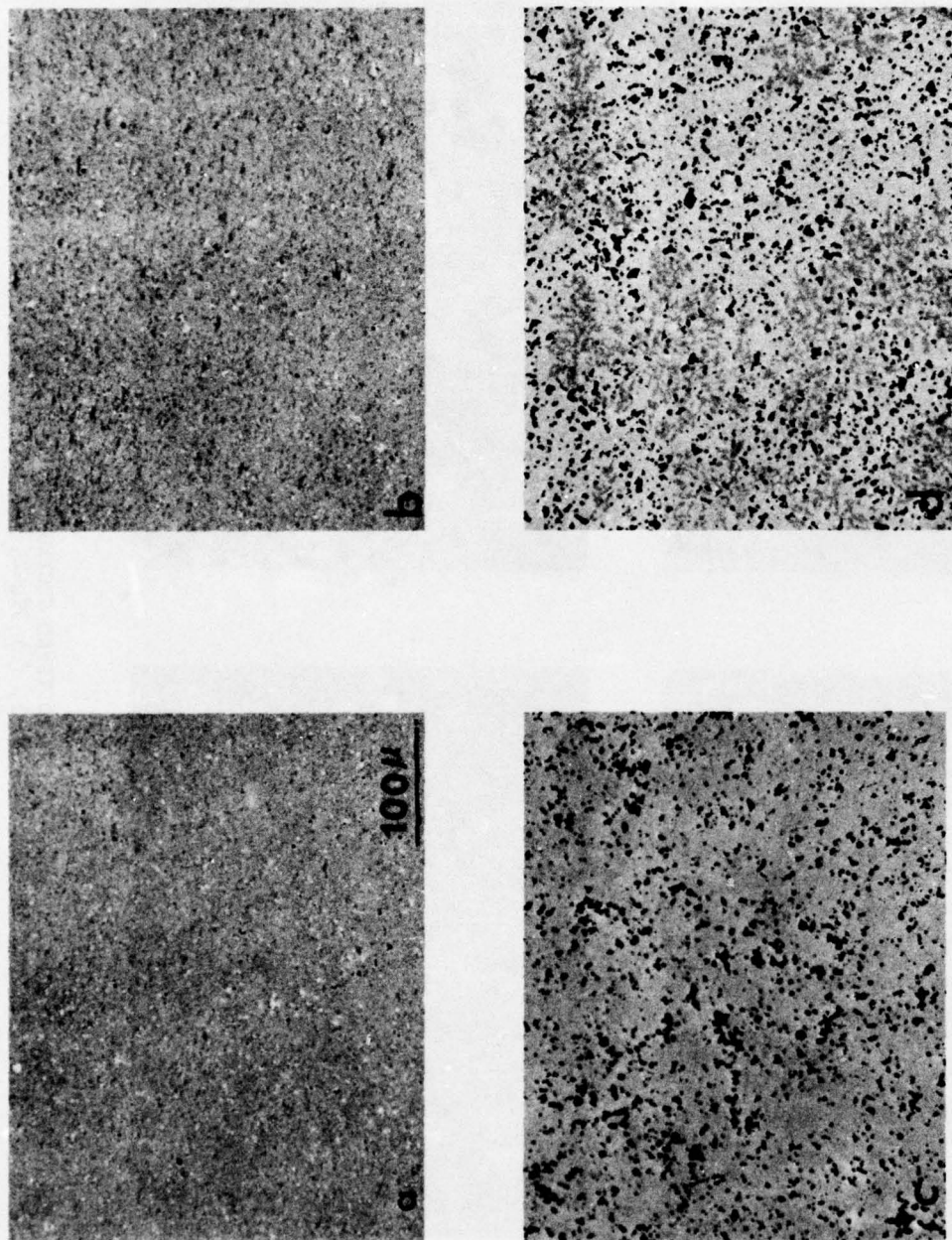


FIGURE 2. OPTICAL MICROGRAPHS OF POLISHED SECTIONS OF Si_3N_4 AND OF VARIOUS SIALONS: (a) NC132, (b) HS130-1, (c) G35A10N-1, (d) SS1/R3-1. 250X

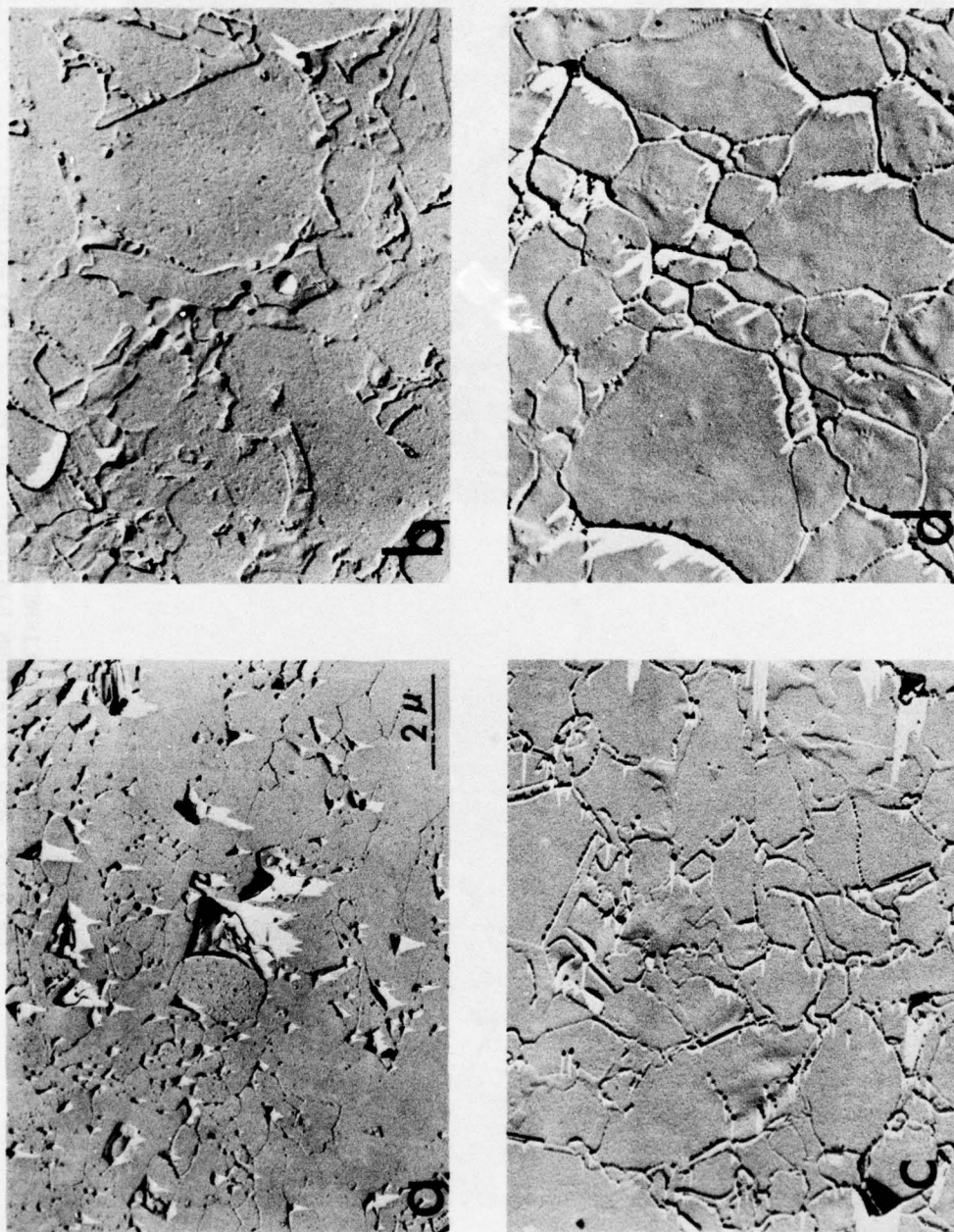


FIGURE 3. MICROSTRUCTURES OF POLISHED AND ETCHED LONGITUDINAL SECTIONS OF Si_3N_4 AND OF VARIOUS SIALONS: (a) HSi_3O , (b) G20A10N-1, (c) 59D-2, (d) 65C-1. $\times 8000$

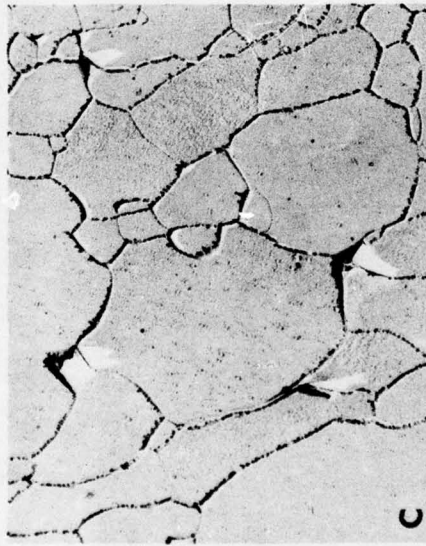
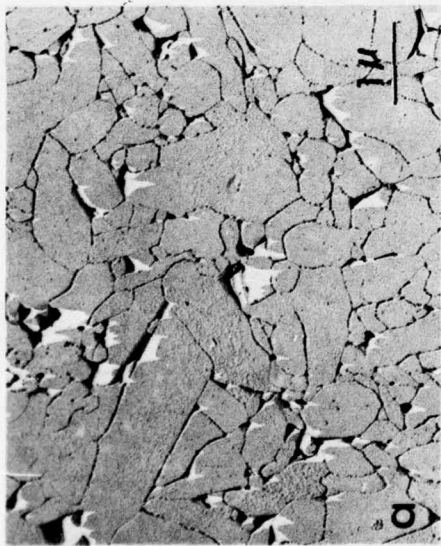
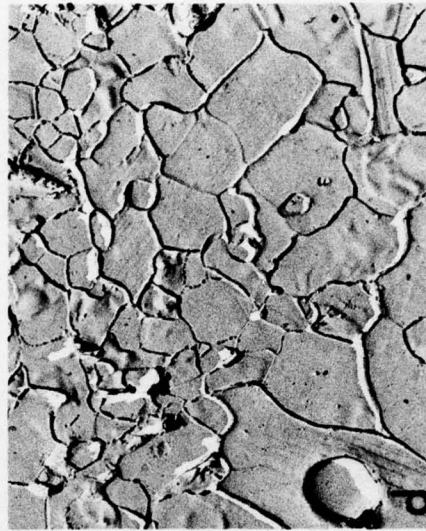
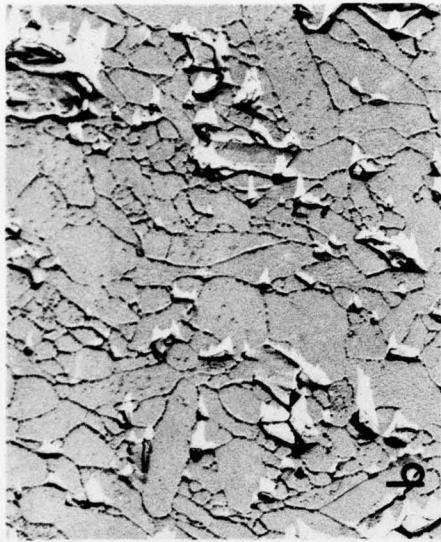


FIGURE 4. MICROSTRUCTURES OF POLISHED AND ETCHED LONGITUDINAL SECTIONS OF Si_3N_4 AND OF VARIOUS SIALONS: (a) NC132, (b) HS130-1, (c) G35AlON-1, (d) SS1/R3-1. 12000X

defined, perhaps as a result of the absence of a silicate grain boundary phase. A better definition of the grain structure of the G20AlON was obtained by replicating a surface which was etched after having cleaved at room temperature (see Figure 5).

The structures of the HS130 and SiAlONs are presented in greater detail in the scanning electron micrographs (SEM) shown in Figure 6. These photos corroborate the light micrograph evidence for high density in the HS130 and G20AlON and increasing porosity in the SiAlON 59D and 65C. The SEM micrographs were taken from transverse sections of the same specimens shown in Figure 1, which had been prepared by fracturing them at room temperature.

The major crystalline phase in each SiAlON composition obtained from Westinghouse was the expanded β' - $\text{Si}_3\text{N}_4(\text{Al}_2\text{O}_3)$ solid solution. Figure 7 includes as-polished microstructures of the four compositions. Phases present in addition to the β' include WC, SiC, Si_2ON_2 (in the 20 w/o composition) α - Al_2O_3 (in the 50 w/o composition) and the unknown X-phase, common to all compositions (dark gray phase). This phase was nearly unresolvable in the 20 w/o composition, but was found to increase from about 10-15 v/o to 20-25 v/o with increasing Al_2O_3 concentration in the 30-50 w/o Al_2O_3 samples⁽¹⁸⁾. The white spots were found to be highly reflecting phases such as WC and Si.

The grain structures obtained after etching (3-10 minutes in 20% NH_4FHF aqueous solution at 180°F) and replicating the surfaces shown in Figure 7 are presented in Figure 8. The 20 w/o Al_2O_3 composition proved most difficult to etch, possibly because it contained a minimum of grain boundary phase. Grain size appears to be fairly uniform for each composition with most grains have a diameter of 0.1 to 1.0 μm .

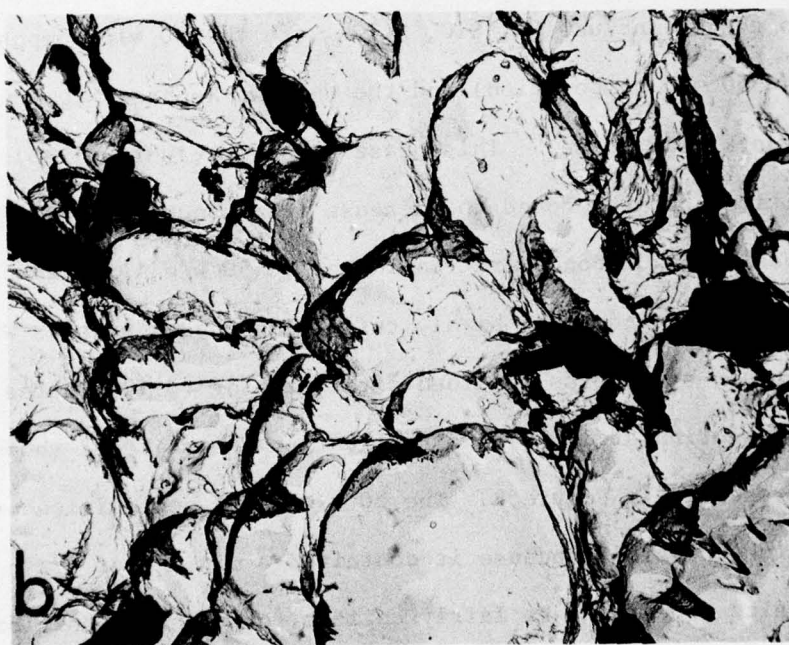
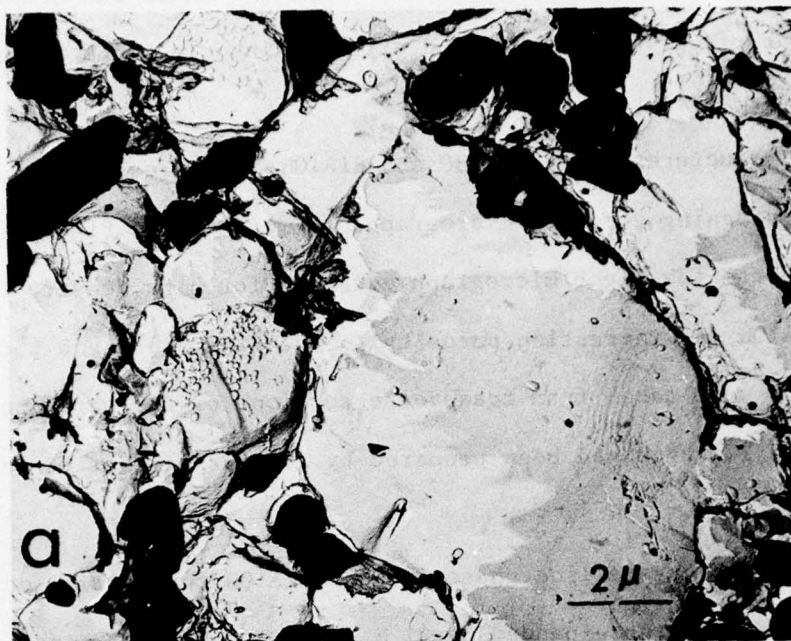


FIGURE 5. MICROSTRUCTURE OF ETCHED FRACTURE SURFACE OF G20A10N, AS-FABRICATED. 8000X

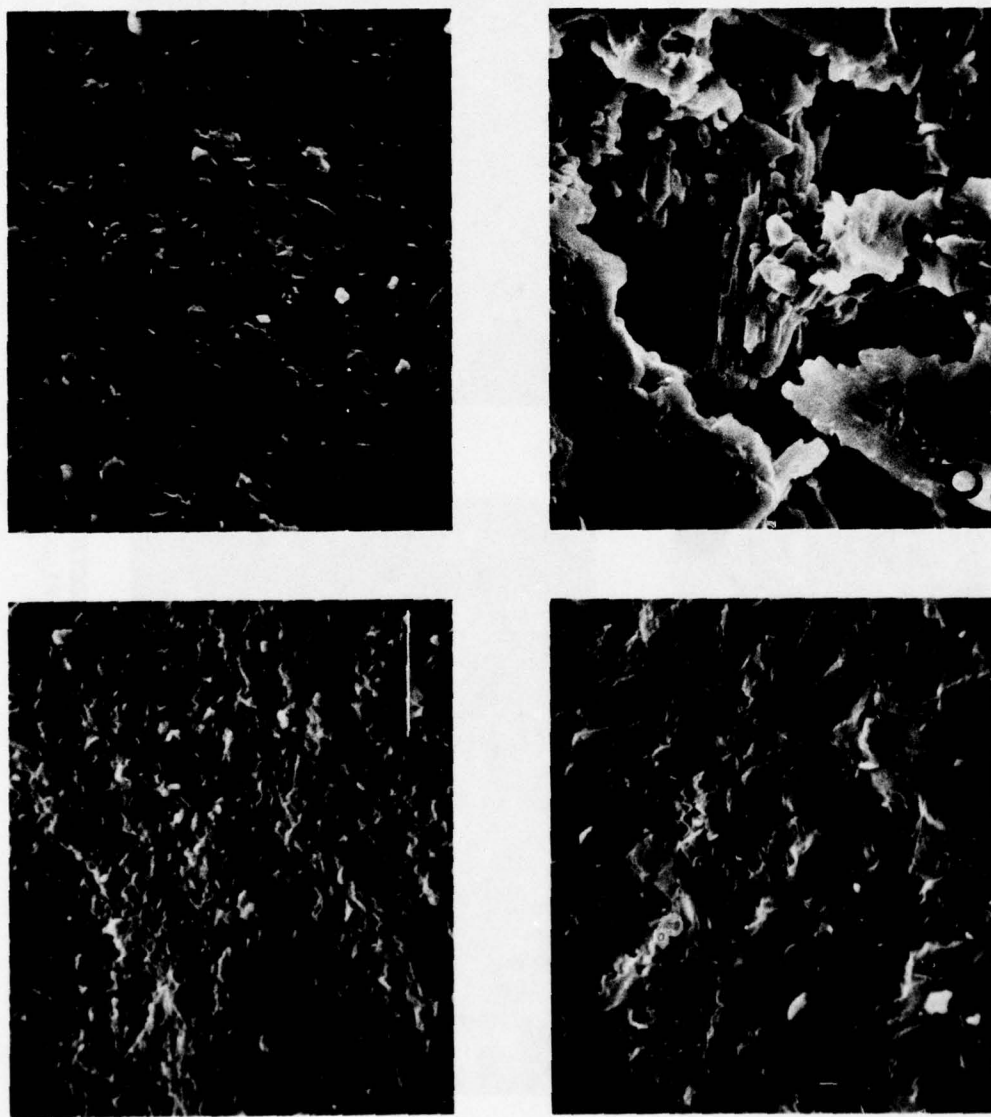


FIGURE 6. SCANNING ELECTRON MICROGRAPHS OF Si_3N_4 AND OF VARIOUS SIALONS: (a) HS130, (b) G20A10N-1, (c) 59D-2, (d) 65C-1. 2000X

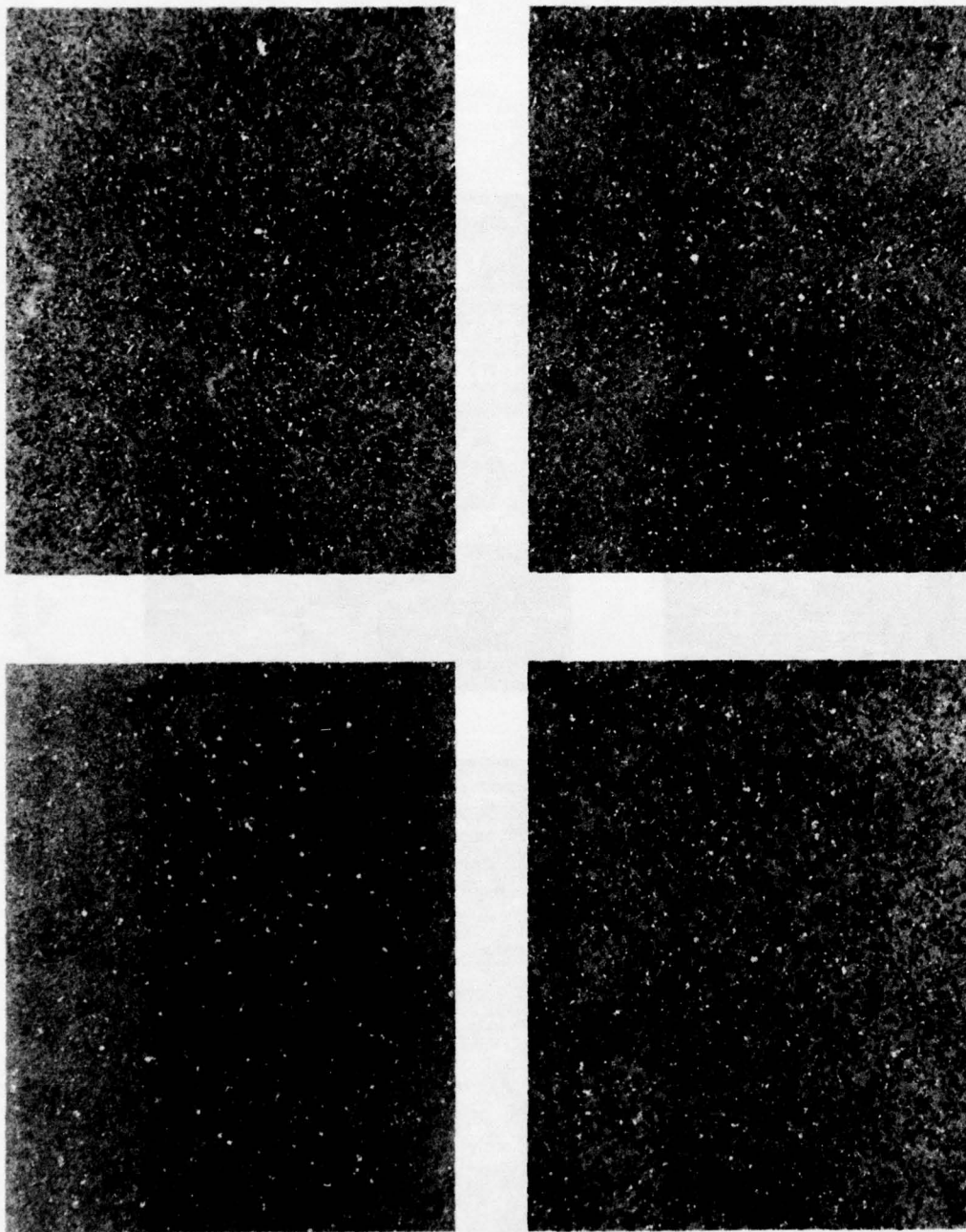


FIGURE 7. OPTICAL MICROGRAPHS OF POLISHED SECTIONS OF VARIOUS SIALONS: (a) 20 w/o Al_2O_3 , (b) 30 w/o Al_2O_3 , (c) 40 w/o Al_2O_3 , and (d) 50 w/o Al_2O_3

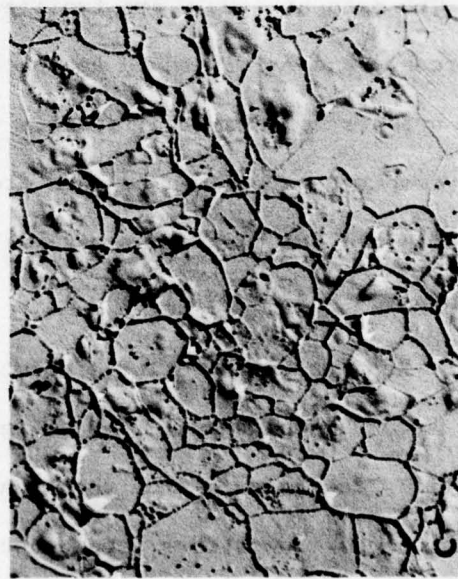


FIGURE 8. MICROSTRUCTURES OF POLISHED AND ETCHED SECTIONS OF VARIOUS SIALONS: (a) 20 w/o Al_2O_3 , (b) 30 w/o Al_2O_3 , (c) 40 w/o Al_2O_3 , and (d) 50 w/o Al_2O_3

Optical micrographs of as-polished surfaces of the three Norton materials NC203, NC340 and NC435 are presented in Figure 9. The general appearance of the NC203 is similar to that of high density hot pressed silicon nitride HS130 and NC132, while the reaction bonded NC350 appears to have the porosity expected of this low density material.

The grain structures obtained after etching (3-10 min in 20% NH_4FHF aqueous solution at 180°F) and replicating the surfaces shown in Figure 9 are presented in Figure 10. The nature of the matrix phase containing particles for NC435 is apparent from Figure 10b.

2. Creep of Silicon-Base Materials

Typical plots of compression creep strain versus time obtained for HS130-1 and SiAlON 59D-1 at 1400°C in air are presented in Figures 11 and 12, respectively. In both cases the data were obtained from stress changes on a single specimen so the strain values are those recorded at the given stress level. The data at 1400°C are typified by small primary creep regimes (tenths of a percent) and fairly rapid approach to minimum creep rate behavior. The HS130-1 appears to have significantly less creep resistance than SiAlON 59D-1 at this temperature, as can be seen from the nearly identical strain-time curves obtained for the former material at 2000 psi and the latter material at 30000 psi.

Results obtained for specimens HS130-1, HS130-2, and HS130-3 tested in air, argon and nitrogen, respectively, are shown in Figure 13. A number of observations can be made from these data. All the results can be best fit by assuming a power law-stress dependence with a stress exponent $n = 2.0$. This is the stress dependence reported previously by Kossowsky for HS130 tested

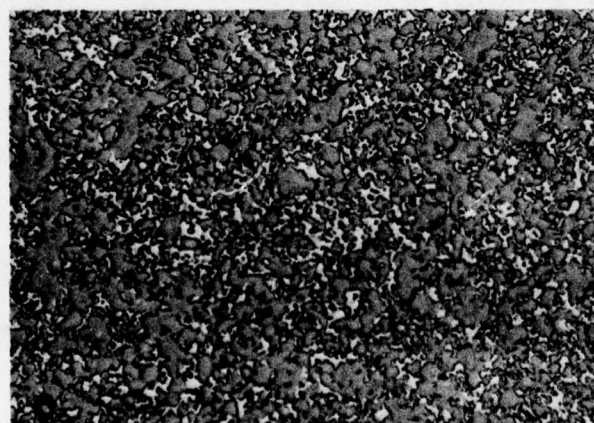
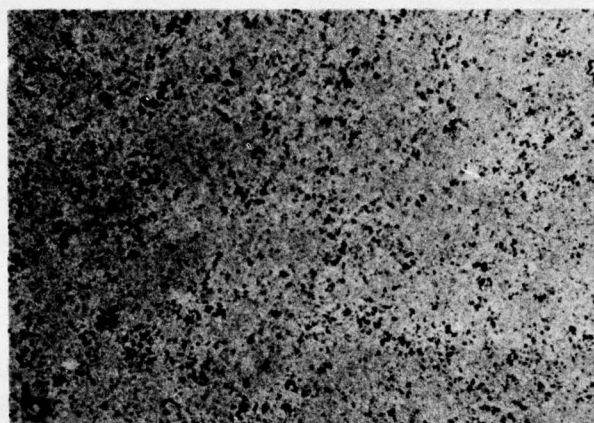
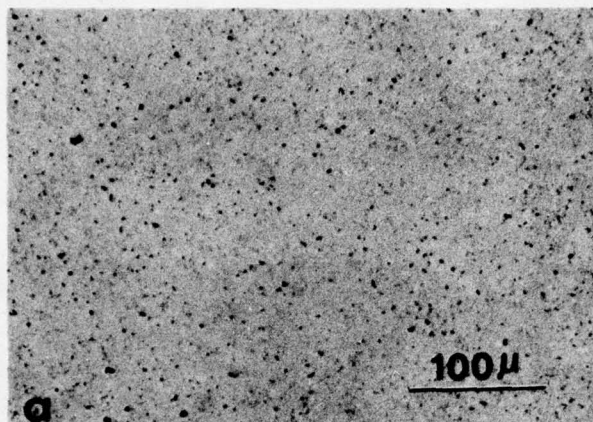


FIGURE 9. MICROSTRUCTURES OF POLISHED SECTIONS OF: (a) NC203, (b) NC350, and (c) NC435. 250X

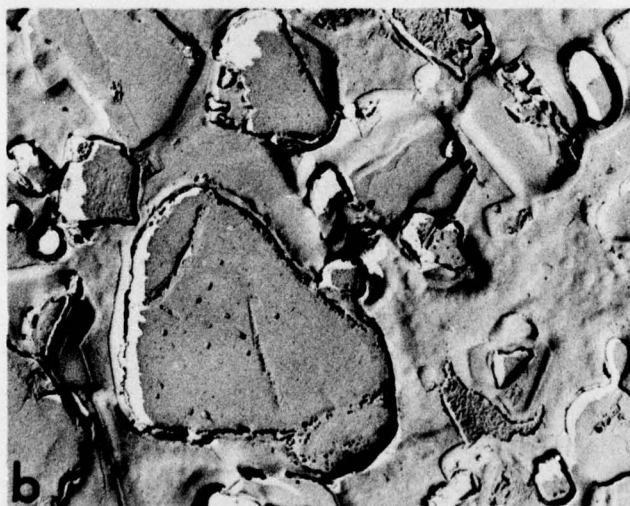


FIGURE 10. MICROSTRUCTURES OF POLISHED AND ETCHED LONGITUDINAL SECTIONS OF: (a) NC203, and (b) NC435. 4500X

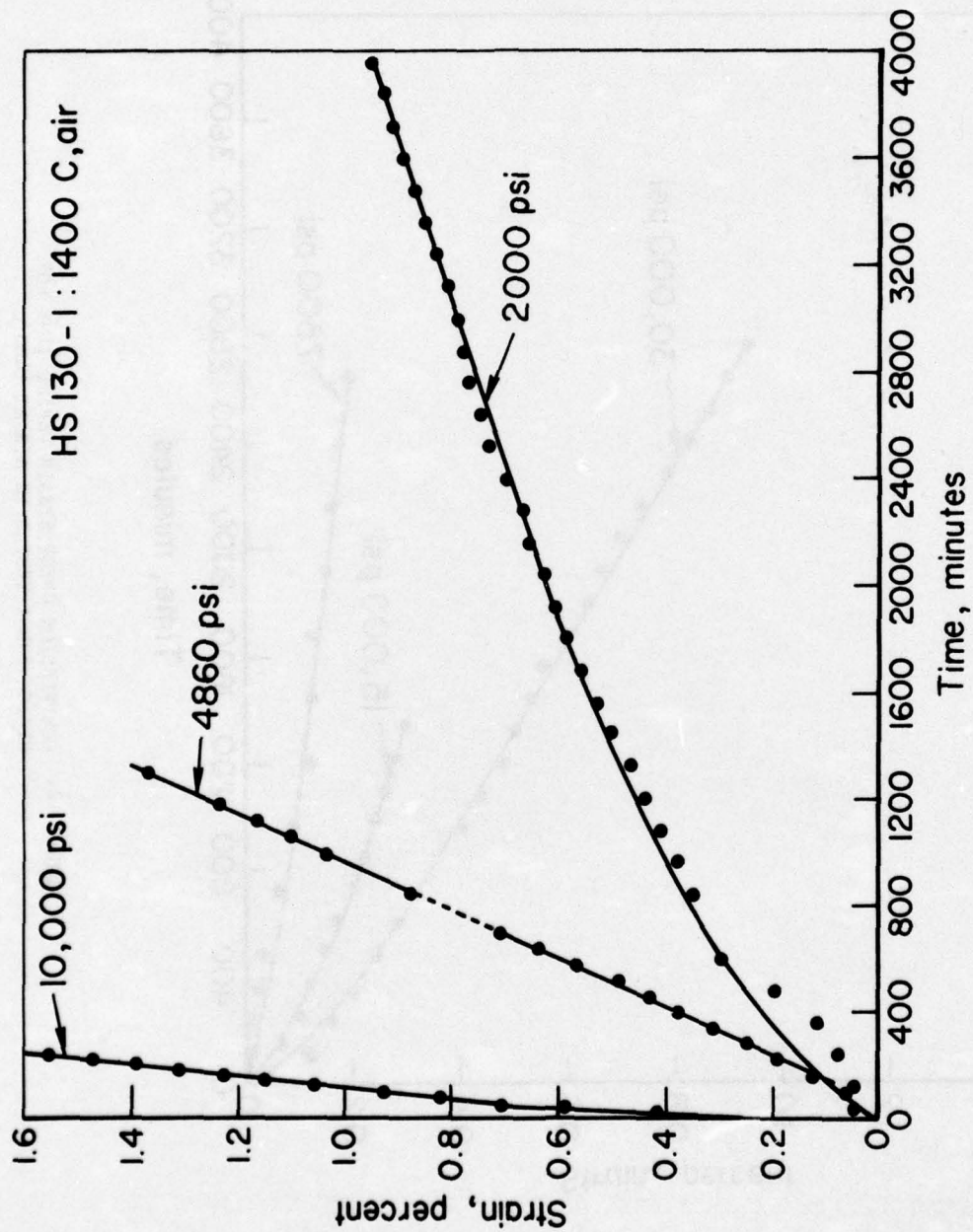


FIGURE 11. COMPRESSION CREEP STRAIN VERSUS TIME FOR
HS130-1 TESTED IN AIR AT 1400°C

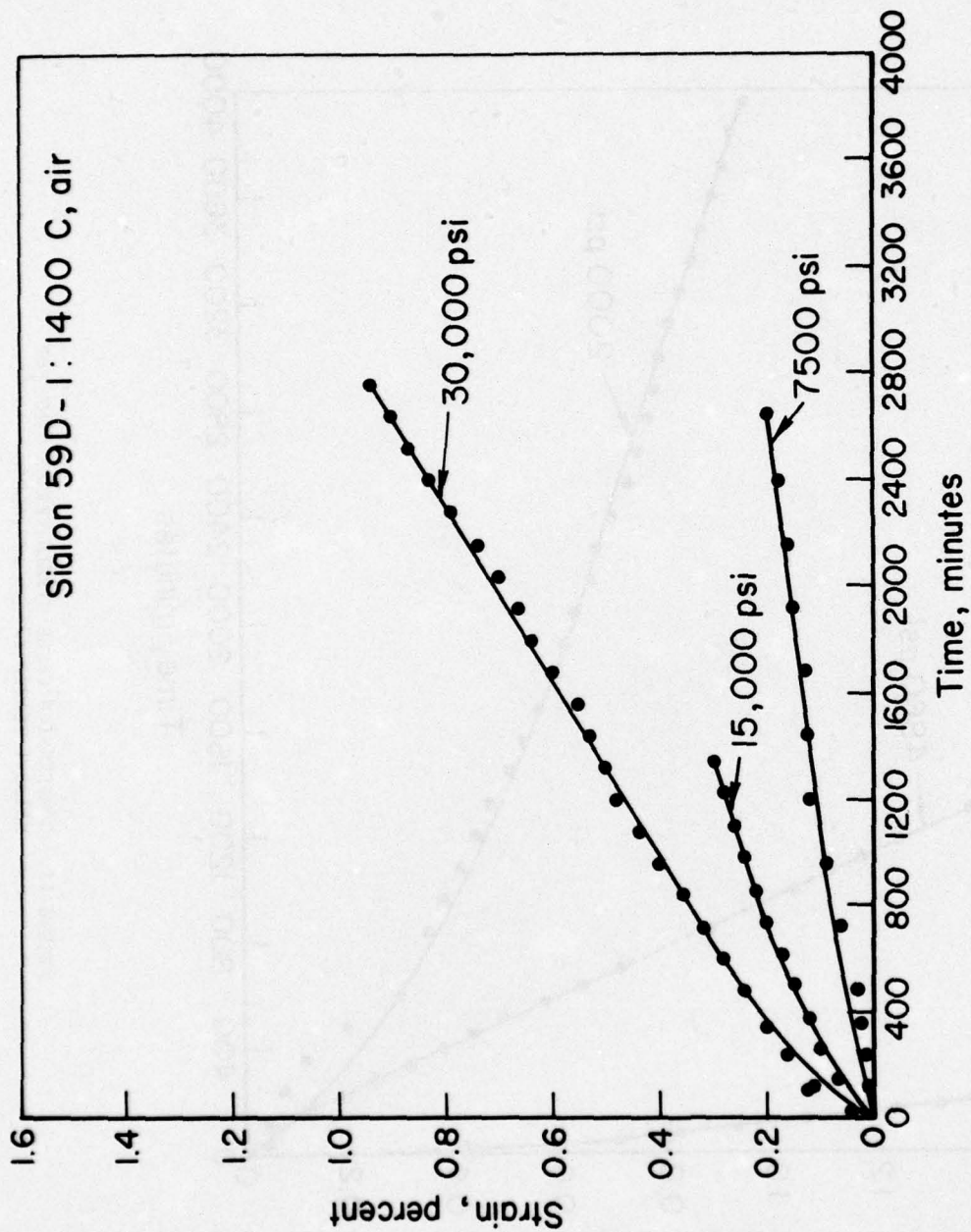


FIGURE 12. COMPRESSION CREEP STRAIN VERSUS TIME FOR
SIALON 59D-1 TESTED IN AIR AT 1400°C

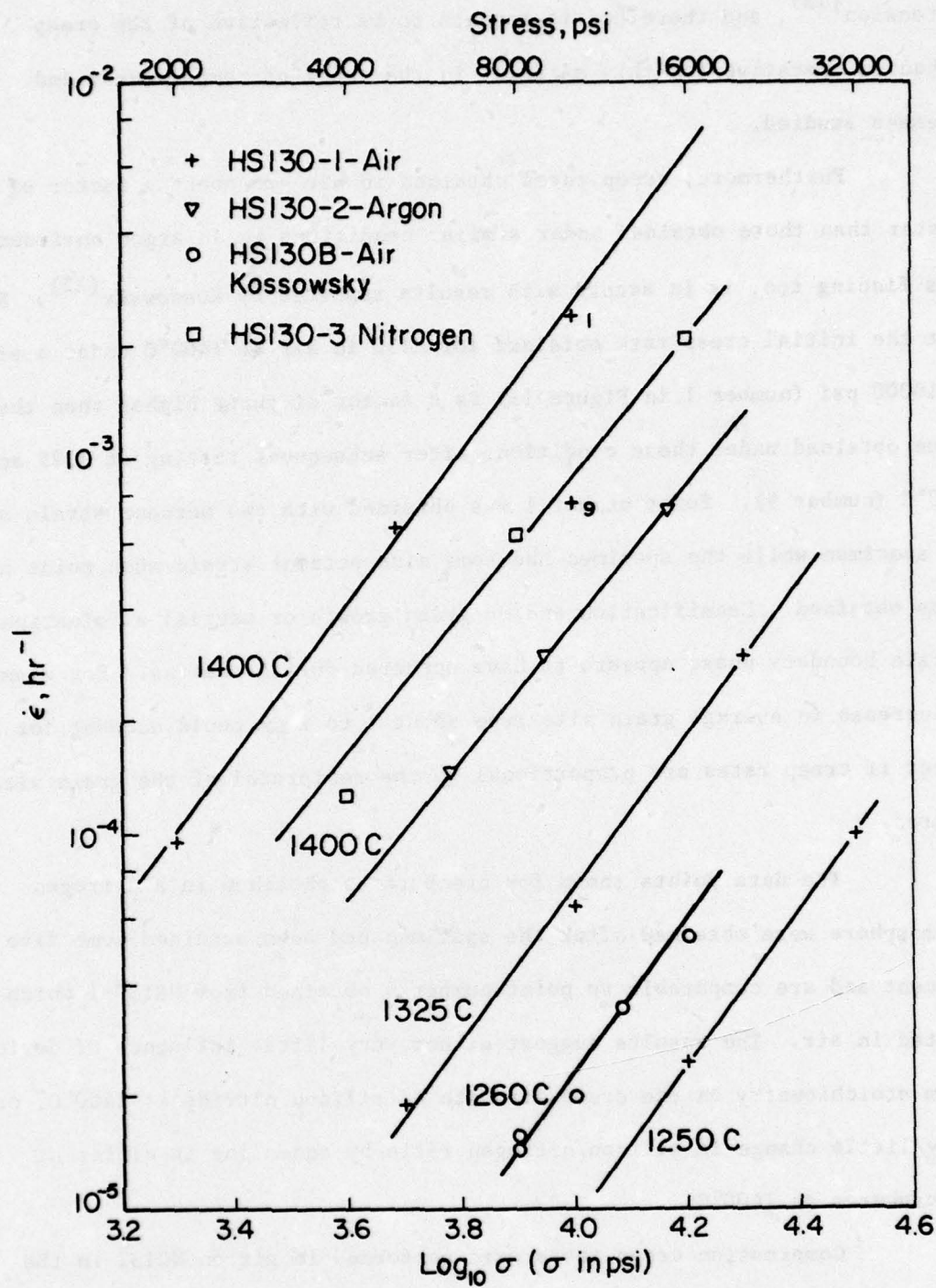


FIGURE 13. STEADY-STATE CREEP RATE VERSUS APPLIED STRESS FOR HS130 TESTED IN AIR, ARGON AND NITROGEN

in tension⁽¹²⁾, and therefore it appears to be reflective of the creep mechanism operative for this material in the range of temperatures and stresses studied.

Furthermore, creep rates obtained in air are about a factor of two greater than those obtained under similar conditions in an argon environment. This finding too, is in accord with results reported by Kossowsky⁽¹²⁾. Note that the initial creep rate obtained for H130 in air at 1400°C under a stress of 10000 psi (number 1 in Figure 13) is a factor of three higher than the value obtained under these conditions after subsequent testing at 1325 and 1250°C (number 9). Point number 1 was obtained with two percent strain on the specimen while the specimen had some nine percent strain when point number 9 was obtained. Densification and/or grain growth or partial elimination of a grain boundary phase appears to have occurred during testing. For example, an increase in average grain size from about 1 to 2 μm could account for this effect if creep rates are proportional to the reciprocal of the grain size squared.

The data points shown for creep rates obtained in a nitrogen atmosphere were obtained after the specimen had been strained some five percent and are comparable to point number 9 obtained from HS130-1 which was tested in air. The results suggest either very little influence of deviation from stoichiometry on the creep strength of silicon nitride at 1400°C, or very little change in silicon/nitrogen ratio by annealing in different atmospheres at 1400°C.

Compression creep tests were performed in air on NC132 in the temperature range of 1250-1400°C at stresses from 2500-40000 psi. In each case a region of primary creep behavior, in which creep rates decrease with time, was followed by a steady-state regime. The steady-state creep rates,

$\dot{\epsilon}$ are plotted as a function of applied stress, σ in Figure 14. The data can be fit by a power law stress dependence where $\dot{\epsilon} \propto \sigma^n$ and the stress exponent $1.8 < n < 2.0$. This value for n is similar to the value obtained for compression creep of HS130, and differs from the linear stress dependency found for the SiAlON materials.

The temperature dependencies for hot-pressed silicon nitride (Norton HS130 and NC132) tested in tension and compression are presented in Figure 15. Included in this figure are tension creep data obtained by Kossowsky et al.⁽¹²⁾ on Norton hot-pressed Si_3N_4 which they designated HS130B. These specimens contained about 0.04 wt % Ca, 0.005 wt % Na, 0.005 wt % K, 0.2 wt % Al, 0.5 wt % Fe and 0.35 wt % Mg. These impurity levels are similar to the concentrations found in the HS130 tested in this study. For example, HS130-1 had 0.03 wt % Ca, 0.2 wt % Al, 0.5 wt % Mg and 0.2 wt % Fe.

Figure 15 shows that the creep activation energies, Q_c , for HS130 and NC132 are similar, as measured either in tension or compression. None of the data are so extensive as to yield a precise value for Q_c , but the values obtained from the data in Figure 15 are 168 ± 5 Kcal/mole. For a given material, creep rates in tension are higher than those measured in compression, but whereas the difference is a factor of three for HS130, for the NC132 there appears to be an increase of several orders of magnitude if the tension data are normalized to 10000 psi. For NC132, tension tests were conducted in vacuum rather than air, and this may have contributed to the difference in observed behavior. However, as will be shown, creep rates for SiAlON 65C were greater in air than in vacuum, therefore the effect observed for NC132 in Figure 15 may be even greater than indicated by the experimental data. Another possible cause of the enhancement in creep rates observed in tension tests is the operation of surface

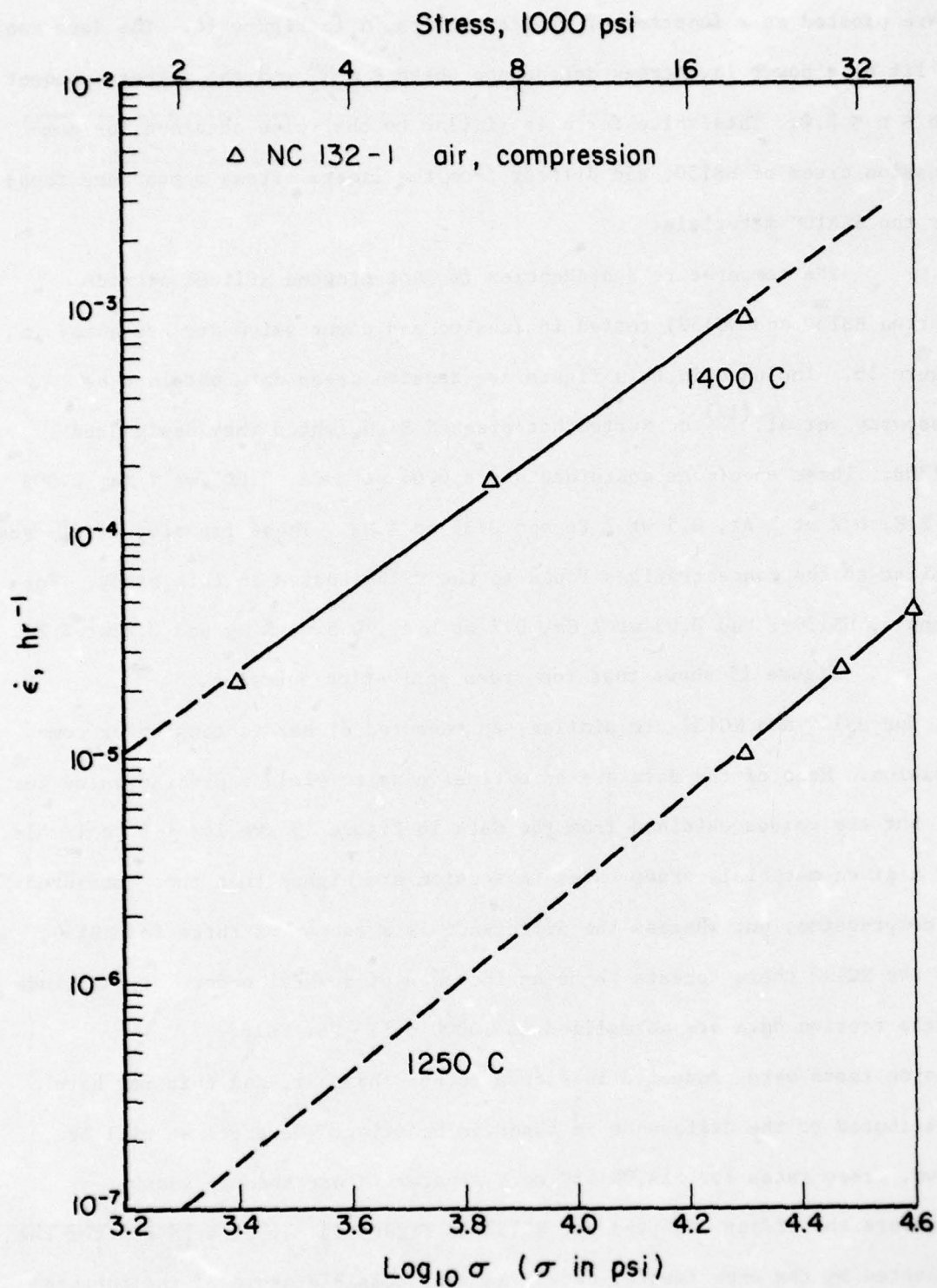


FIGURE 14. STEADY-STATE CREEP RATE VERSUS APPLIED STRESS
FOR NORTON HOT-PRESSED Si_3N_4 TESTED IN AIR

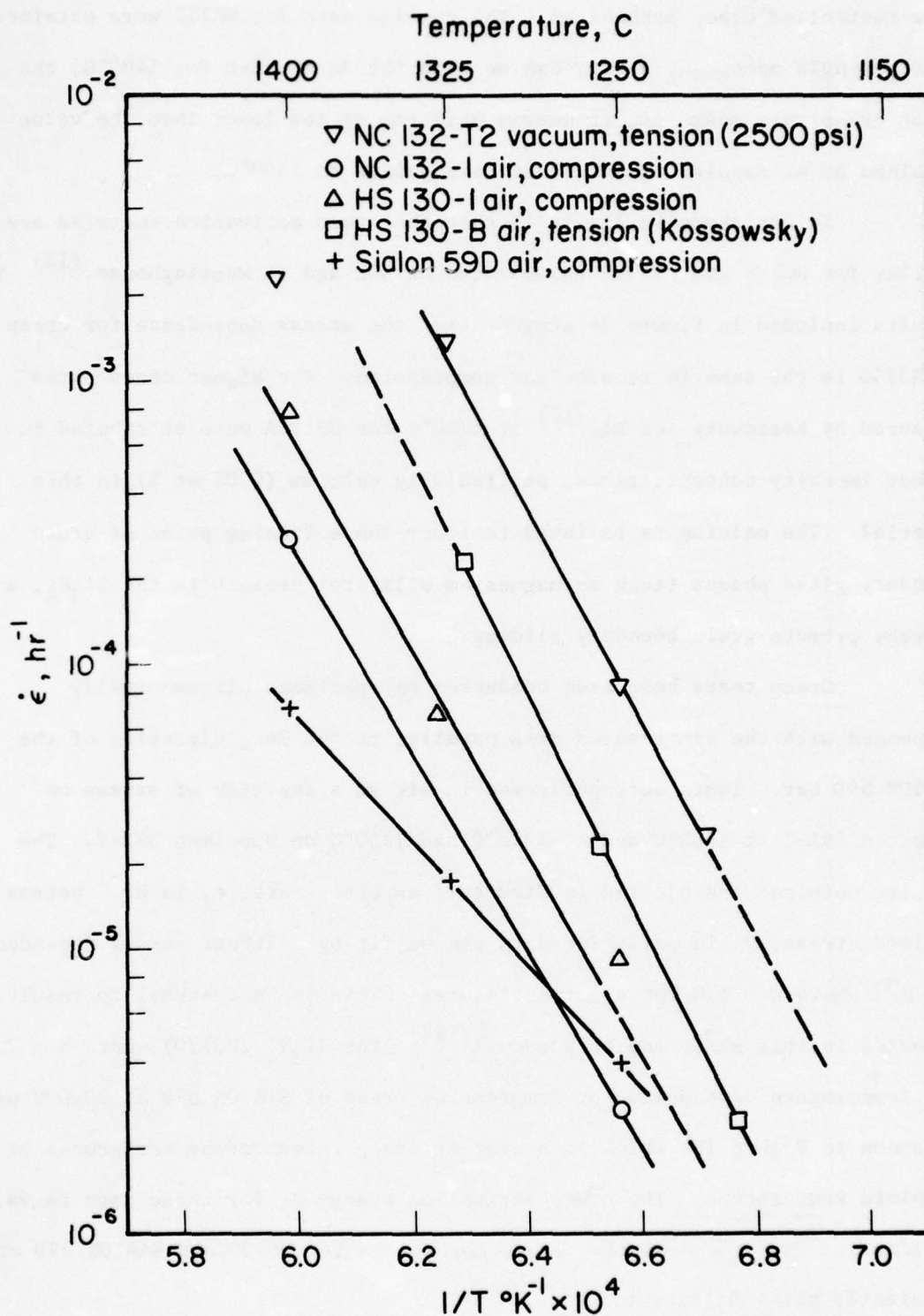


FIGURE 15. STEADY-STATE CREEP RATE VERSUS RECIPROCAL ABSOLUTE TEMPERATURE FOR HOT PRESSED Si_3N_4 (NC 132 AND HS 130) and SIALON 59D TESTED AT 10000 PSI

flaw controlled creep mechanisms. The tension data for NC132 were obtained from a single specimen, and as can be seen the data point for 1400°C, the first creep rate measured, is nearly a factor of ten lower than the value obtained by extrapolating the other data points to 1400°C.

It was shown in Figure 15 that the creep activation energies are similar for NC132 and HS130, as measured at BCL and at Westinghouse.⁽¹²⁾ The results included in Figure 16 suggest that the stress dependence for creep of HS130 is the same in tension and compression. The higher creep rates measured by Kossowsky et al.⁽¹²⁾ at 1260°C for HS130A were attributed to higher impurity concentrations, particularly calcium (0.07 wt %), in this material. The calcium is believed to lower the softening point of grain boundary glass phases (such as magnesium silicate) present in the Si_3N_4 , and thereby promote grain boundary sliding.

Creep tests have been conducted on specimens ultrasonically trepanned with the compression axis parallel to the long direction of the SiAlON 59D bar. Tests were performed in air as a function of stress on specimen 59D-1 at 1400°C and at 1325°C and 1250°C on specimen 59D-2. The results obtained are plotted in Figure 17 as creep rate, $\dot{\epsilon}$, in hr^{-1} versus applied stress, σ , in psi. The data can be fit by a linear stress dependence $\dot{\epsilon} \propto \sigma^n$, where $n = 1.0$ for all temperatures. This is in contrast to results reported in this study and by Kossowsky⁽¹²⁾ for Si_3N_4 (HS130) where $n \approx 2.0$. The temperature dependence for compression creep of SiAlON 59D at 20,000 psi is shown in Figure 18, which is a plot of creep rates versus reciprocal of the absolute temperature. The creep activation energy Q_c for these data is 94.1 kcal/mole. Thus the operative creep mechanisms for HS130 and SiAlON 59D are apparently quite different.

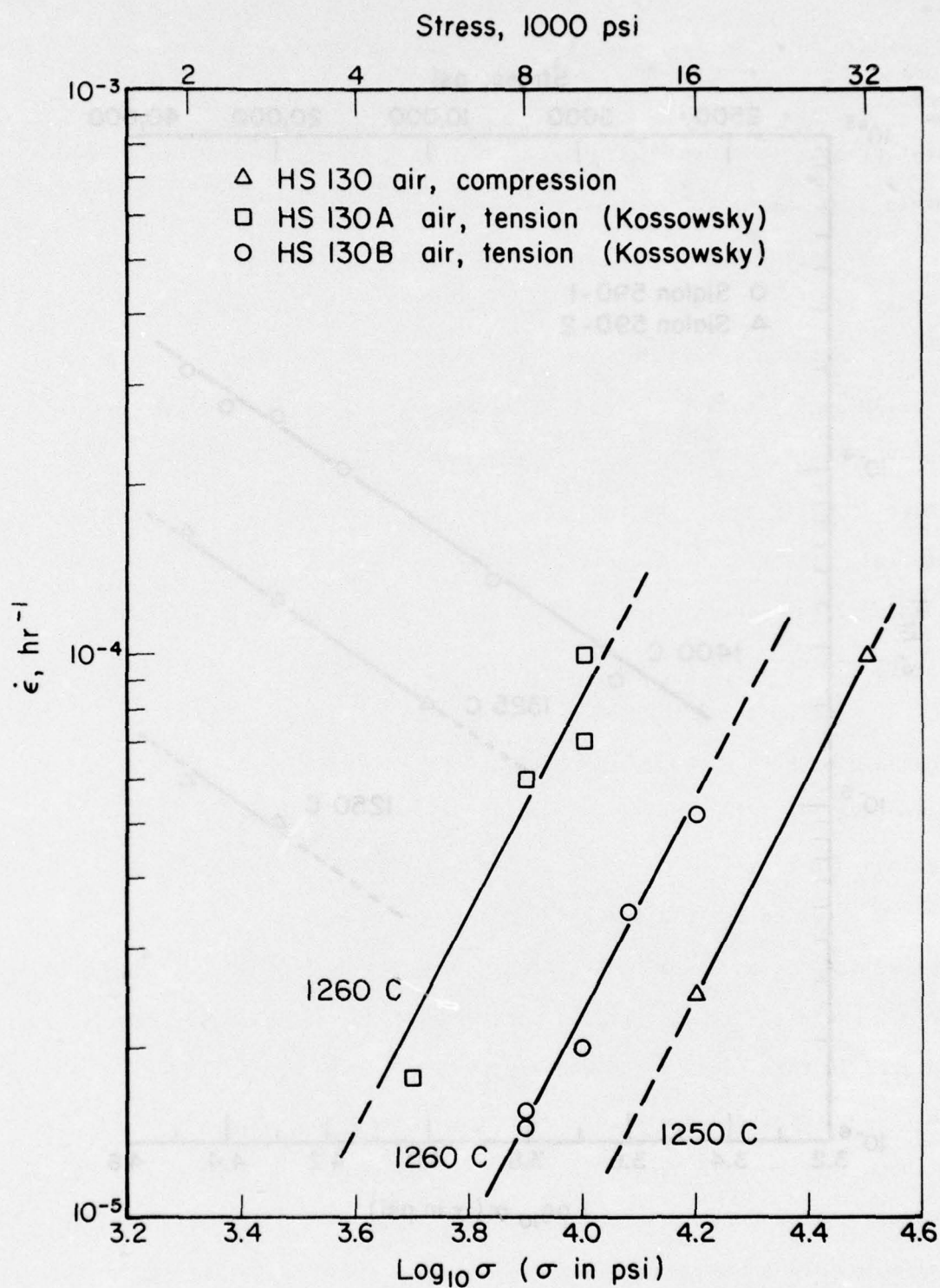


FIGURE 16. STEADY-STATE CREEP RATE VERSUS APPLIED STRESS FOR HS 130

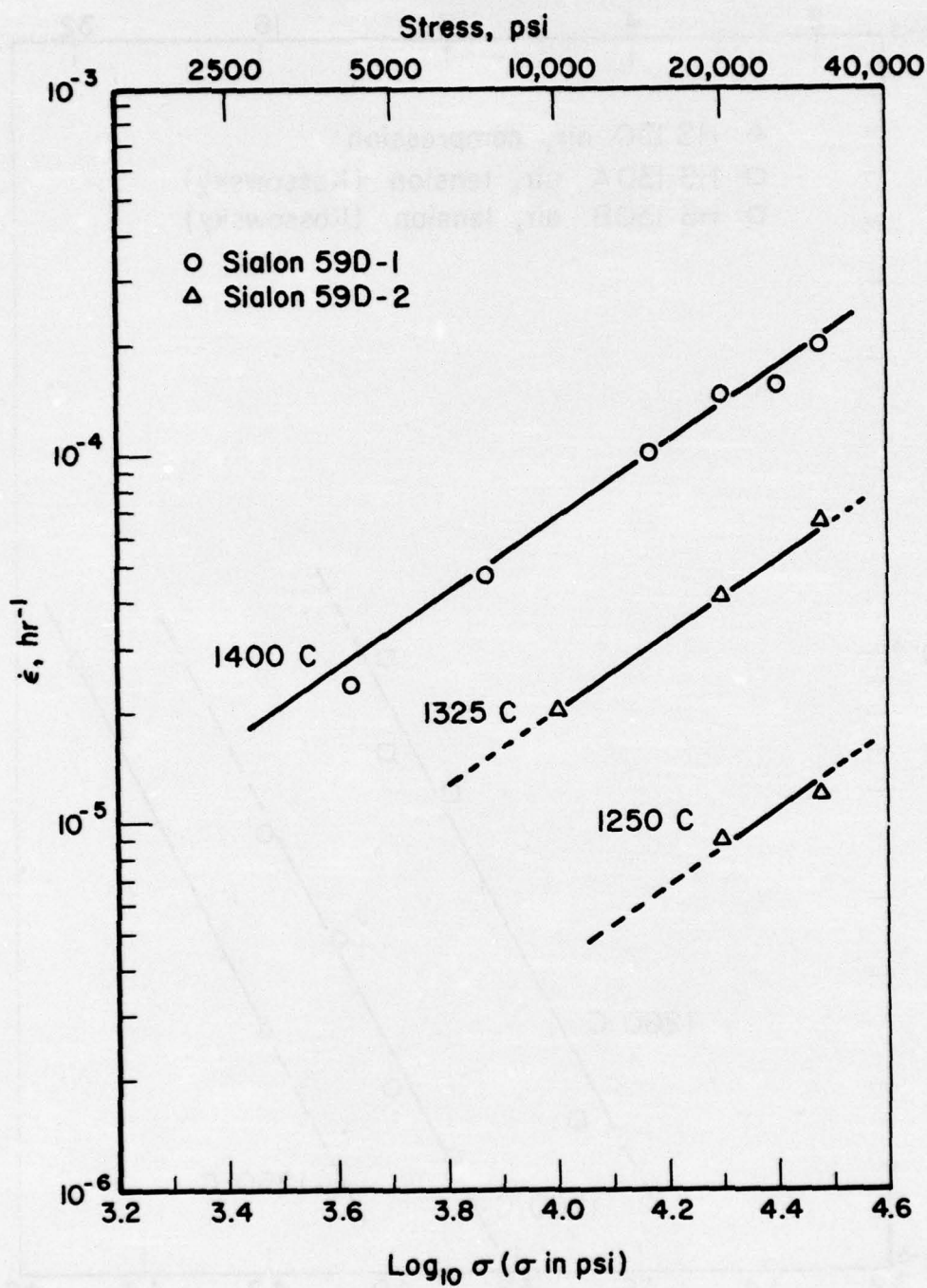


FIGURE 17. STEADY-STATE CREEP RATE VERSUS APPLIED STRESS
FOR SIALON 59D TESTED IN AIR

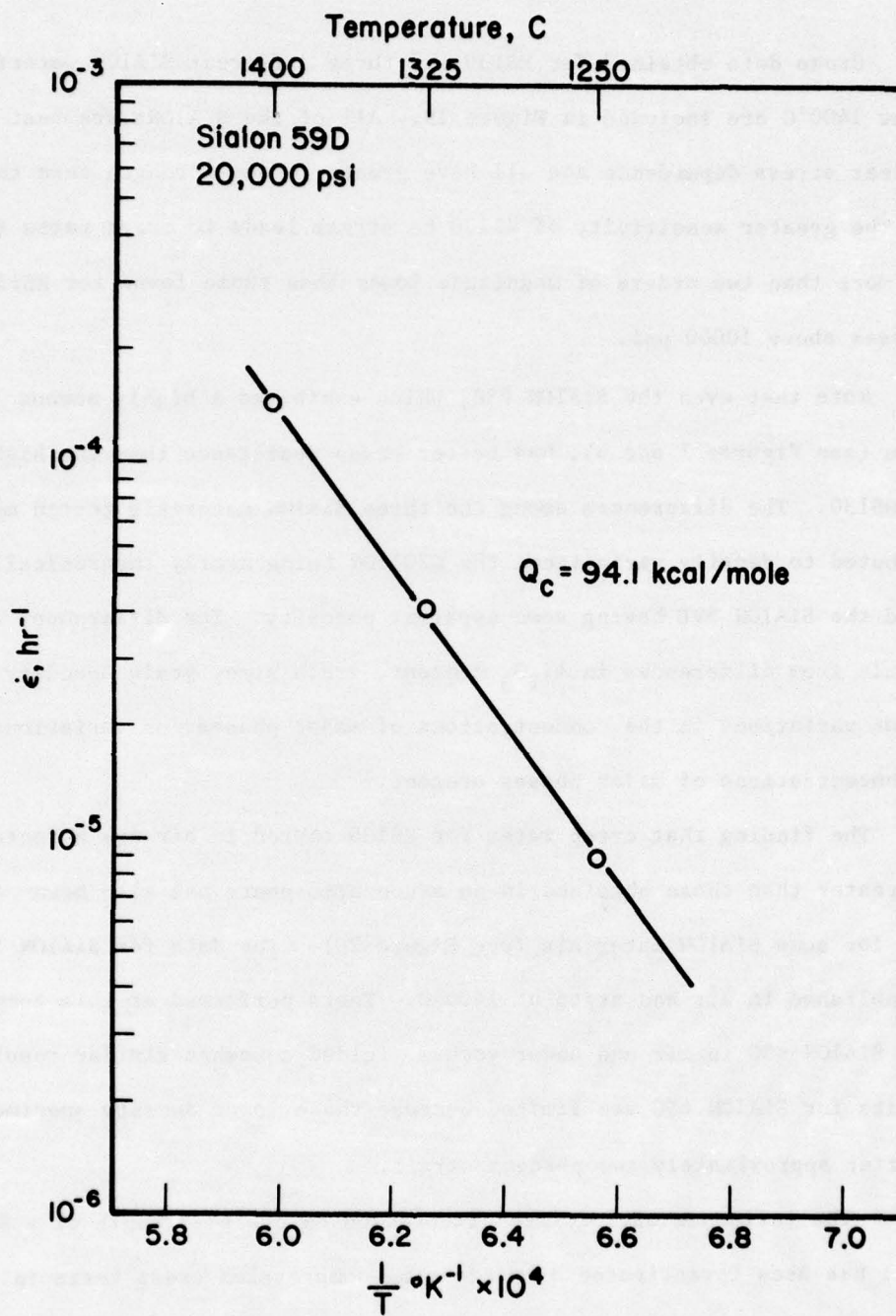


FIGURE 18. STEADY-STATE CREEP RATE VERSUS RECIPROCAL ABSOLUTE TEMPERATURE FOR SIALON 59D TESTED IN AIR, DATA NORMALIZED TO 20,000 PSI

Creep data obtained for HS130 and three different SiAlON materials in air at 1400°C are included in Figure 19. All of the SiAlONs are best fit by a linear stress dependence and all have greater creep strength than the HS130. The greater sensitivity of HS130 to stress leads to creep rates for G20AlON more than two orders of magnitude lower than those found for HS130 at stresses above 10000 psi.

Note that even the SiAlON 65C, which exhibited a highly porous structure (see Figures 1 and 6), had better creep resistance than the high-density HS130. The differences among the three SiAlON materials tested may be attributed to density variations, the G20AlON being nearly theoretically dense and the SiAlON 59D having some apparent porosity. The differences may also result from differences in Al_2O_3 content, grain size, grain boundary phases, or variations in the concentrations of major phases, or variations in the concentrations of major phases present.

The finding that creep rates for HS130 tested in air are a factor of two greater than those obtained in an argon atmosphere has also been observed for some SiAlON materials (see Figure 20). The data for SiAlON 59D were established in air and argon at 1400°C. Tests performed at this temperature on SiAlON 65C in air and under vacuum yielded somewhat similar results. The results for SiAlON 65C are limited because these lower density specimens failed after approximately two percent strain.

The influence of specimen orientation on creep strength of a SiAlON material has been investigated by performing compression creep tests in air on samples of SiAlON 65C taken with the compression axis parallel or transverse to the long dimension of the sintered billet. At 1400°C (see Figure 21), creep rates for transverse specimens were about seventy percent higher than those measured in the longitudinal specimens.

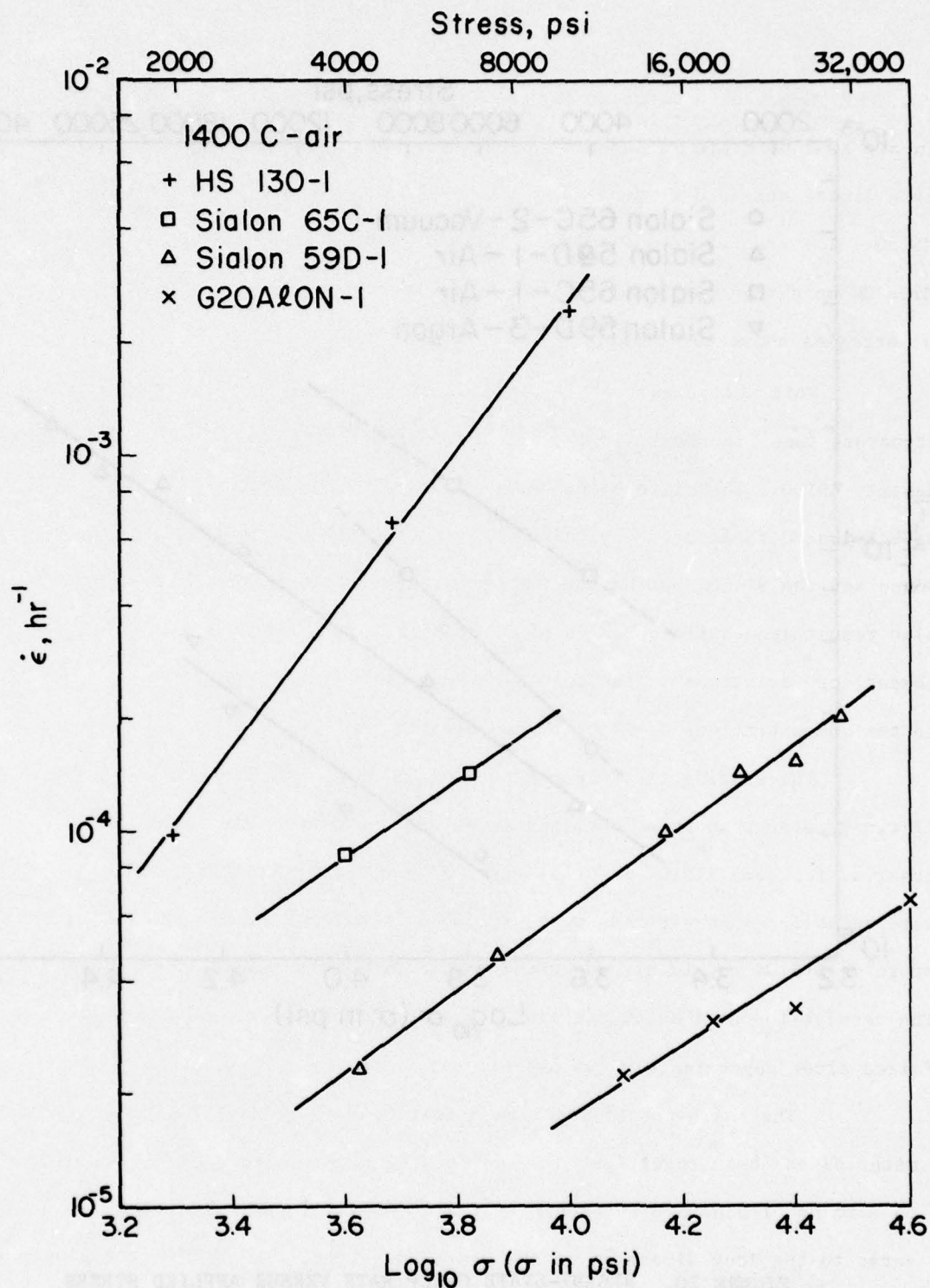


FIGURE 19. COMPARISON OF CREEP DATA OBTAINED AS A FUNCTION OF STRESS AT 1400°C IN AIR FOR HS130 AND THREE DIFFERENT SIALON MATERIALS

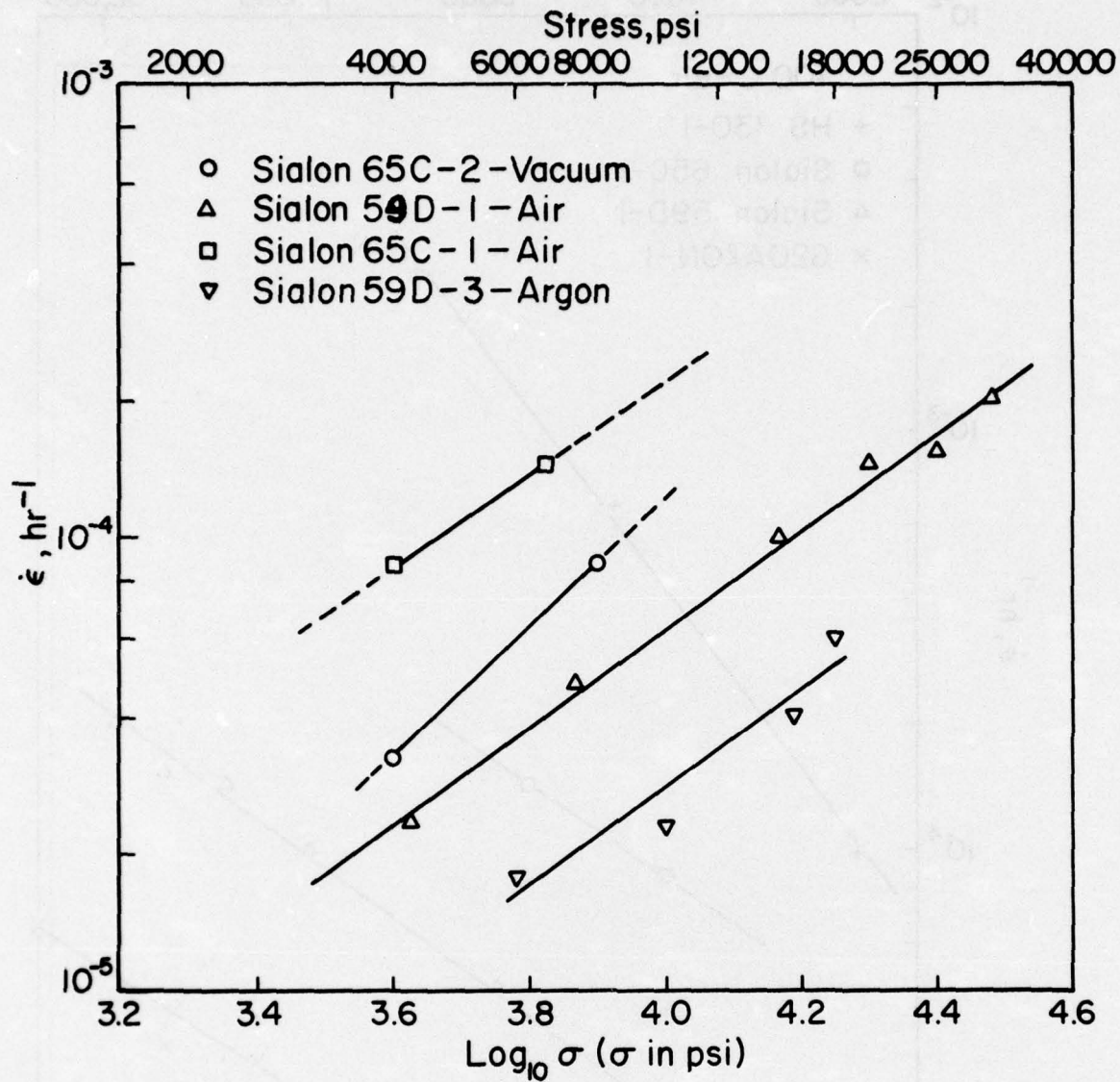


FIGURE 20. STEADY-STATE CREEP RATE VERSUS APPLIED STRESS FOR SIALONS 59D AND 65C TESTED IN AIR, ARGON, AND VACUUM AT 1400°C

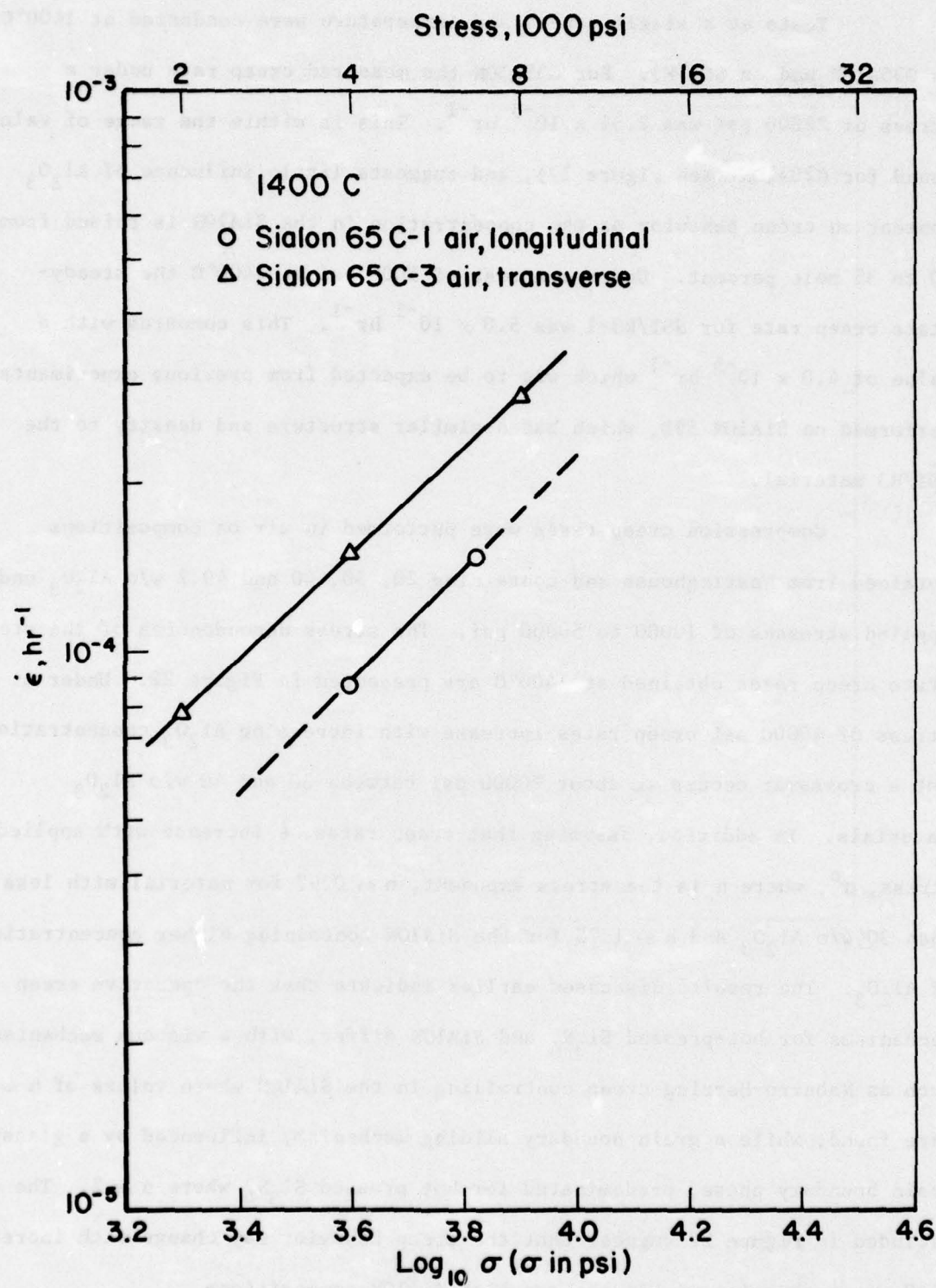


FIGURE 21. STEADY-STATE CREEP RATE VERSUS APPLIED STRESS FOR SIALON 65 C

Tests at a single stress and temperature were conducted at 1400°C on G35AlON and on SSI/R3. For G35AlON the measured creep rate under a stress of 22000 psi was $2.35 \times 10^{-5} \text{ hr}^{-1}$. This is within the range of values found for G20AlON (see Figure 19), and suggests little influence of Al_2O_3 content on creep behavior as the concentration in the SiAlON is raised from 20 to 35 mole percent. Under a stress of 5000 psi at 1400°C the steady-state creep rate for SSI/R3-1 was $5.0 \times 10^{-5} \text{ hr}^{-1}$. This compares with a value of $4.0 \times 10^{-5} \text{ hr}^{-1}$ which was to be expected from previous experiments performed on SiAlON 59D, which had a similar structure and density to the SSI/R3 material.

Compression creep tests were performed in air on compositions obtained from Westinghouse and containing 20, 30, 40 and 49.2 w/o Al_2O_3 under applied stresses of 10000 to 50000 psi. The stress dependencies of the steady-state creep rates obtained at 1400°C are presented in Figure 22. Under a stress of 40000 psi creep rates increase with increasing Al_2O_3 concentration but a crossover occurs at about 20000 psi between 30 and 40 w/o Al_2O_3 materials. In addition, assuming that creep rates, $\dot{\epsilon}$ increase with applied stress, σ^n , where n is the stress exponent, $n \approx 0.97$ for material with less than 30 w/o Al_2O_3 and $n \approx 1.75$ for the SiAlON containing higher concentrations of Al_2O_3 . The results discussed earlier indicate that the operative creep mechanisms for hot-pressed Si_3N_4 and SiAlON differ, with a viscous mechanism such as Nabarro-Herring creep controlling in the SiAlON where values of $n \approx 1$ were found, while a grain boundary sliding mechanism, influenced by a glassy grain boundary phase, predominated for hot pressed Si_3N_4 where $n \approx 2$. The data included in Figure 22 suggest that the creep behavior may change with increasing Al_2O_3 concentration within the range of SiAlON compositions.

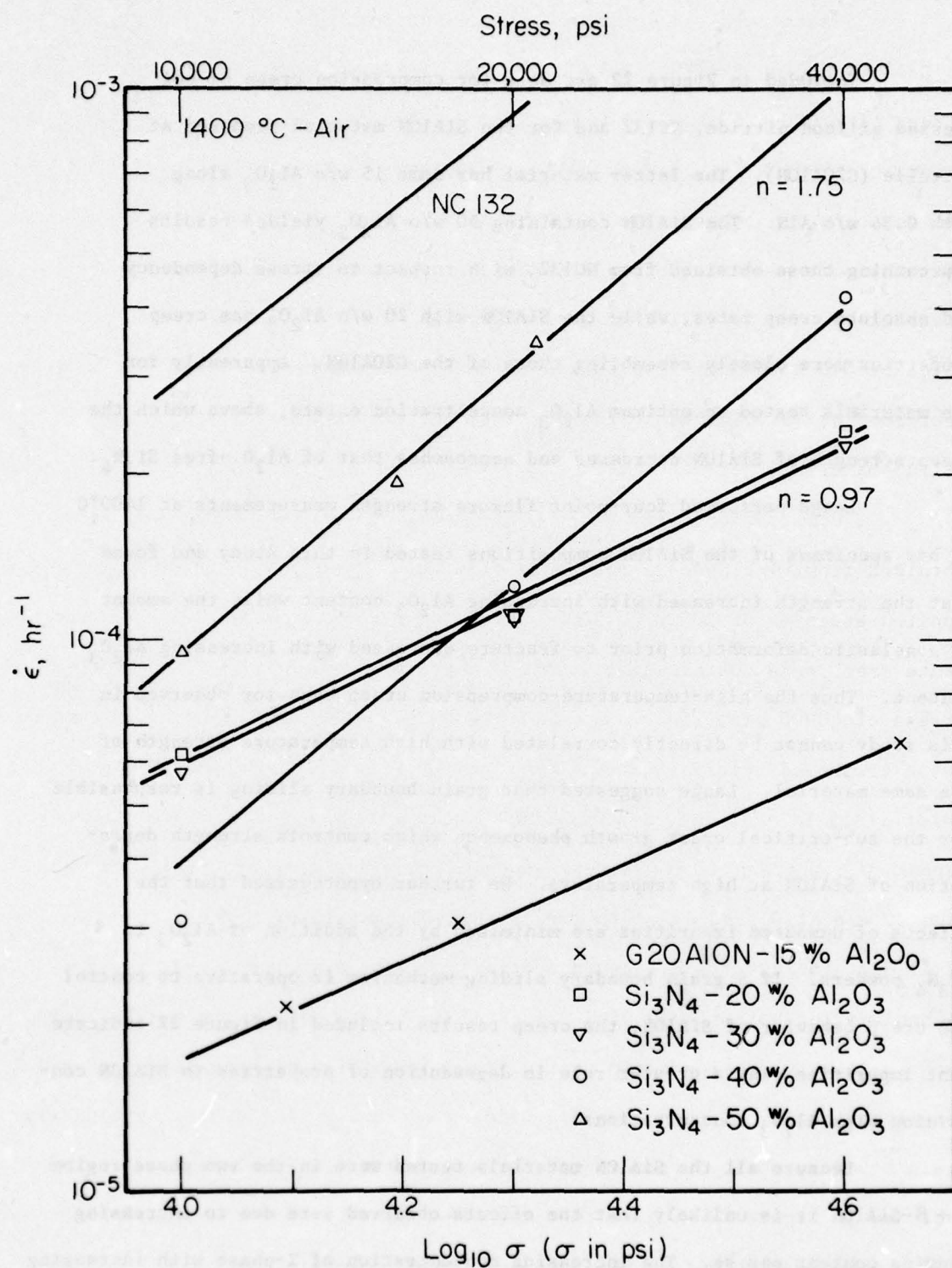


FIGURE 22. STEADY-STATE CREEP RATE VERSUS APPLIED STRESS FOR HOT PRESSED Si₃N₄ AND FOR VARIOUS SiAlON COMPOSITIONS

Included in Figure 22 are data for compression creep of hot pressed silicon nitride, NC132 and for the SiAlON material prepared at Battelle (G20AlON). The latter material has some 15 w/o Al_2O_3 along with 0.34 w/o AlN. The SiAlON containing 50 w/o Al_2O_3 yielded results approaching those obtained from NC132, with respect to stress dependency and absolute creep rates, while the SiAlON with 20 w/o Al_2O_3 has creep properties more closely resembling those of the G20AlON. Apparently for the materials tested an optimum Al_2O_3 concentration exists, above which the creep strength of SiAlON decreases and approaches that of Al_2O_3 -free Si_3N_4 .

Lange performed four-point flexure strength measurements at 1400°C on bar specimens of the SiAlON compositions tested in this study and found that the strength increased with increasing Al_2O_3 content while the amount of nonelastic deformation prior to fracture decreased with increasing Al_2O_3 content. Thus the high-temperature-compression creep behavior observed in this study cannot be directly correlated with high temperature strength of the same material. Lange suggested that grain boundary sliding is responsible for the sub-critical crack growth phenomenon which controls strength degradation of SiAlON at high temperature. He further hypothesized that the effects of unwanted impurities are minimized by the addition of Al_2O_3 to Si_3N_4 powders. If a grain boundary sliding mechanism is operative to control the creep behavior of SiAlON, the creep results included in Figure 22 indicate that impurities play a greater role in degradation of properties in SiAlON containing high Al_2O_3 concentrations.

Because all the SiAlON materials tested were in the two phase region $\text{X} + \beta$ -SiAlON it is unlikely that the effects observed were due to increasing alumina content per se. The increasing concentration of X-phase with increasing Al_2O_3 concentration offers a ready explanation for the results obtained. If

this phase has a low melting temperature, we can assume that the composition containing high concentrations of X-phase would be more likely to evidence low creep strength, resulting from operation of a grain boundary sliding mechanism.

Creep rates for SiAlON containing 40 and 50 w/o Al_2O_3 have also been obtained at 1325°C. These results, presented in Figure 23 suggest that the stress dependence is independent of temperature in the range of 1325-1400°C. The data yield an creep activation energy Q_c , of 152 ± 9 kcal/mole. This compares with values of 168 ± 5 kcal/mole and 130-150 kcal/mole obtained in this study, and by Kossowsky⁽²²⁾ for hot-pressed Si_3N_4 , which had a stress dependence similar to that for the 40 and 50 w/o Al_2O_3 specimens, and a value of 94 kcal/mole obtained in this study for SiAlON materials which had a linear stress dependence. This is further evidence of the apparent similarity of mechanisms for creep of hot-pressed Si_3N_4 and high-alumina concentration SiAlON as compared with the SiAlON containing 20 w/o Al_2O_3 or less.

Data obtained for Westinghouse SiAlON containing 30 w/o Al_2O_3 at 1325 and 1400°C are included in Figure 24. These data yield a creep activation energy of 158 kcal/mole, a value similar to those found for hot-pressed Si_3N_4 and for the Westinghouse SiAlON with 40 and 50 w/o Al_2O_3 . In all previous activation energy determinations for SiAlON materials, where the linear stress dependence was observed, the activation energy for creep was found to be approximately 95 kcal/mole. For SiAlON prepared by Westinghouse, the same diffusion mechanism apparently controls the creep processes which yield linear and power law stress dependencies.

Results for the limited tests conducted on reaction bonded silicon nitride (NC350), hot-pressed silicon carbide (NC203) and fine-grained densified silicon carbide (NC435), are presented in Figure 25, along with results discussed earlier for hot-pressed silicon nitride (NC132) and the best SiAlON material G20AlON. The NC350 has compressive creep strength superior

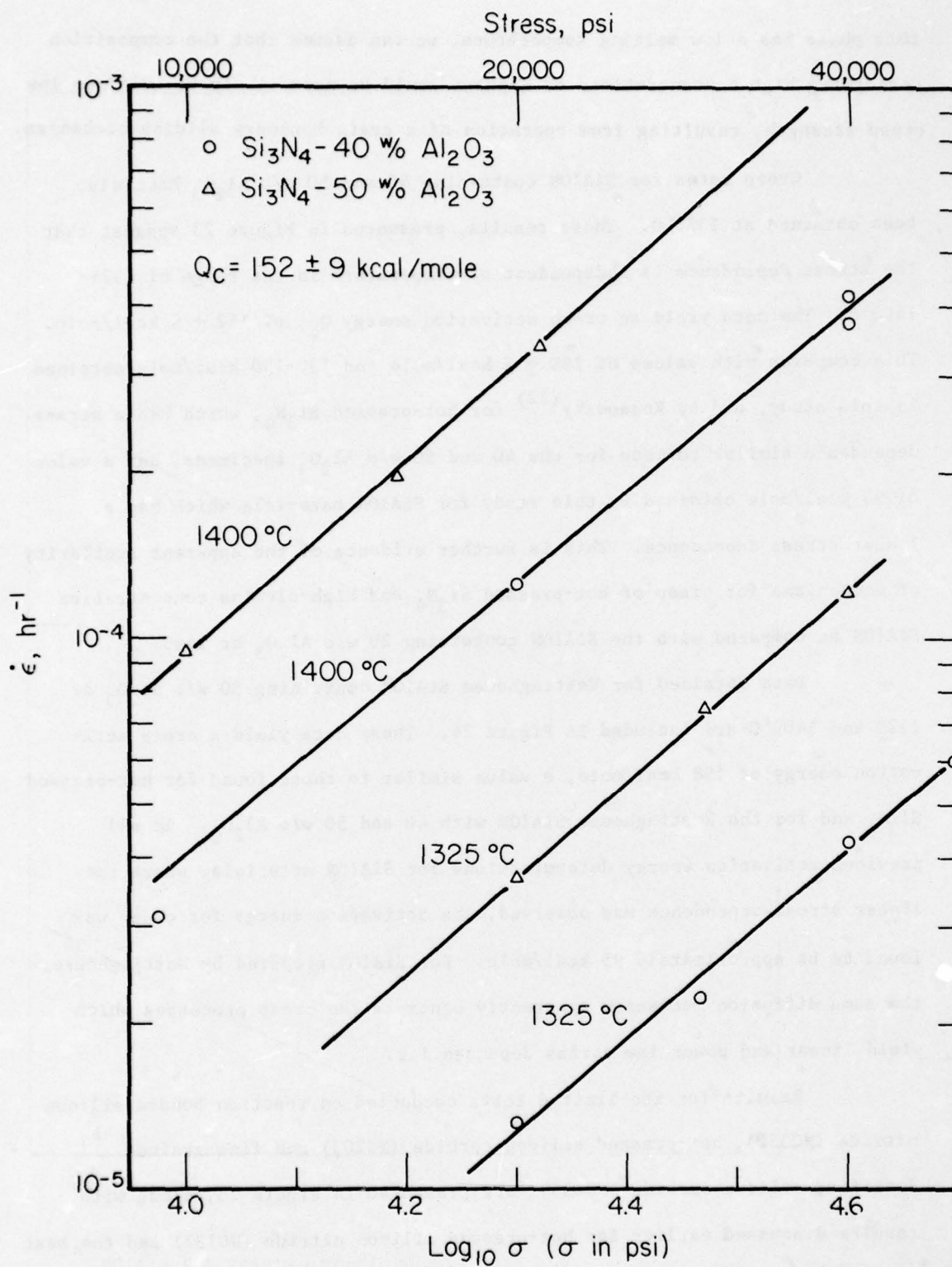


FIGURE 23. STEADY STATE CREEP RATE VERSUS APPLIED STRESS FOR SIALON CONTAINING 40 AND 50 w/o Al_2O_3 .

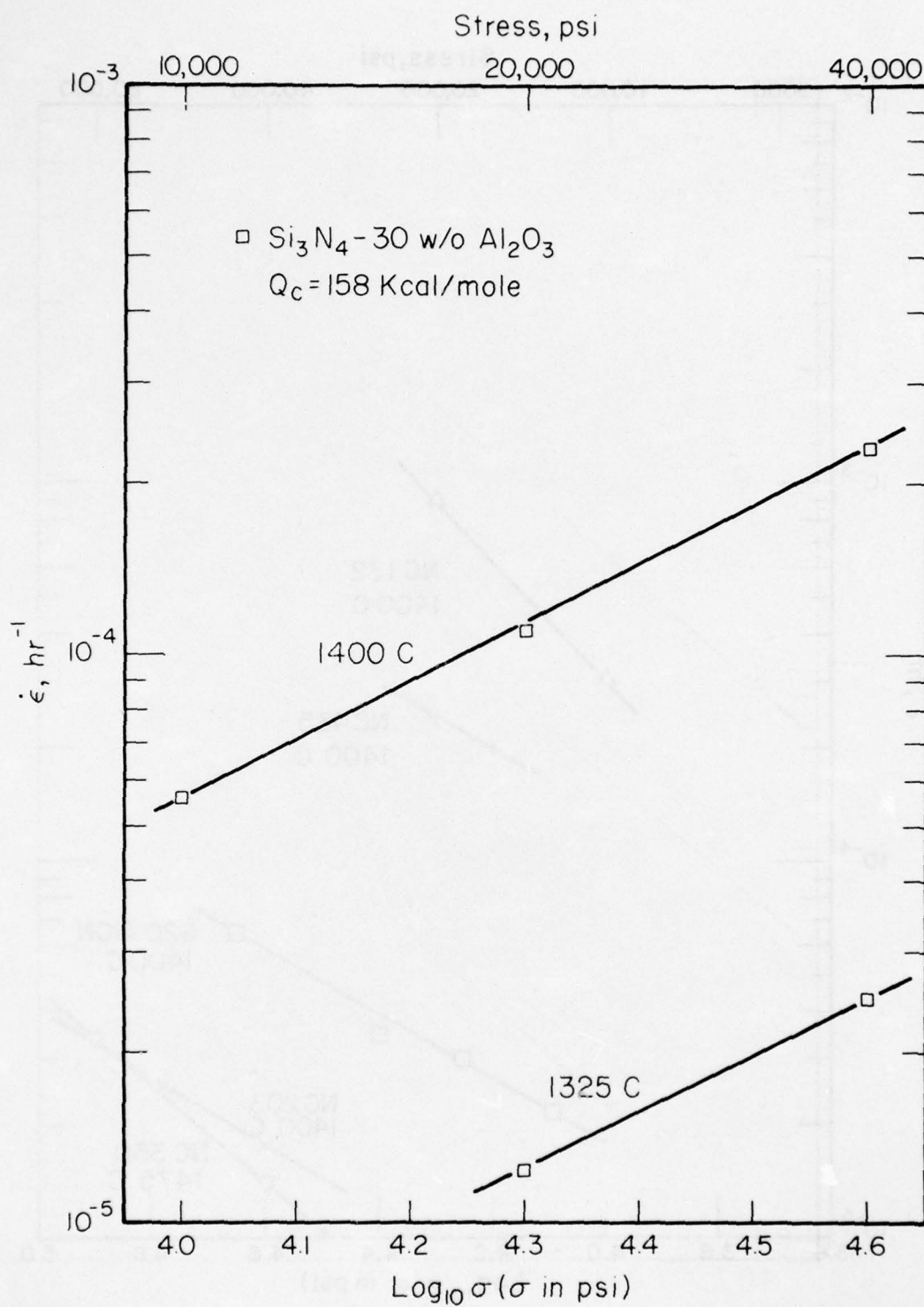


FIGURE 24. STEADY-STATE CREEP RATE VERSUS APPLIED STRESS FOR SiAlON CONTAINING 30 W/O Al_2O_3

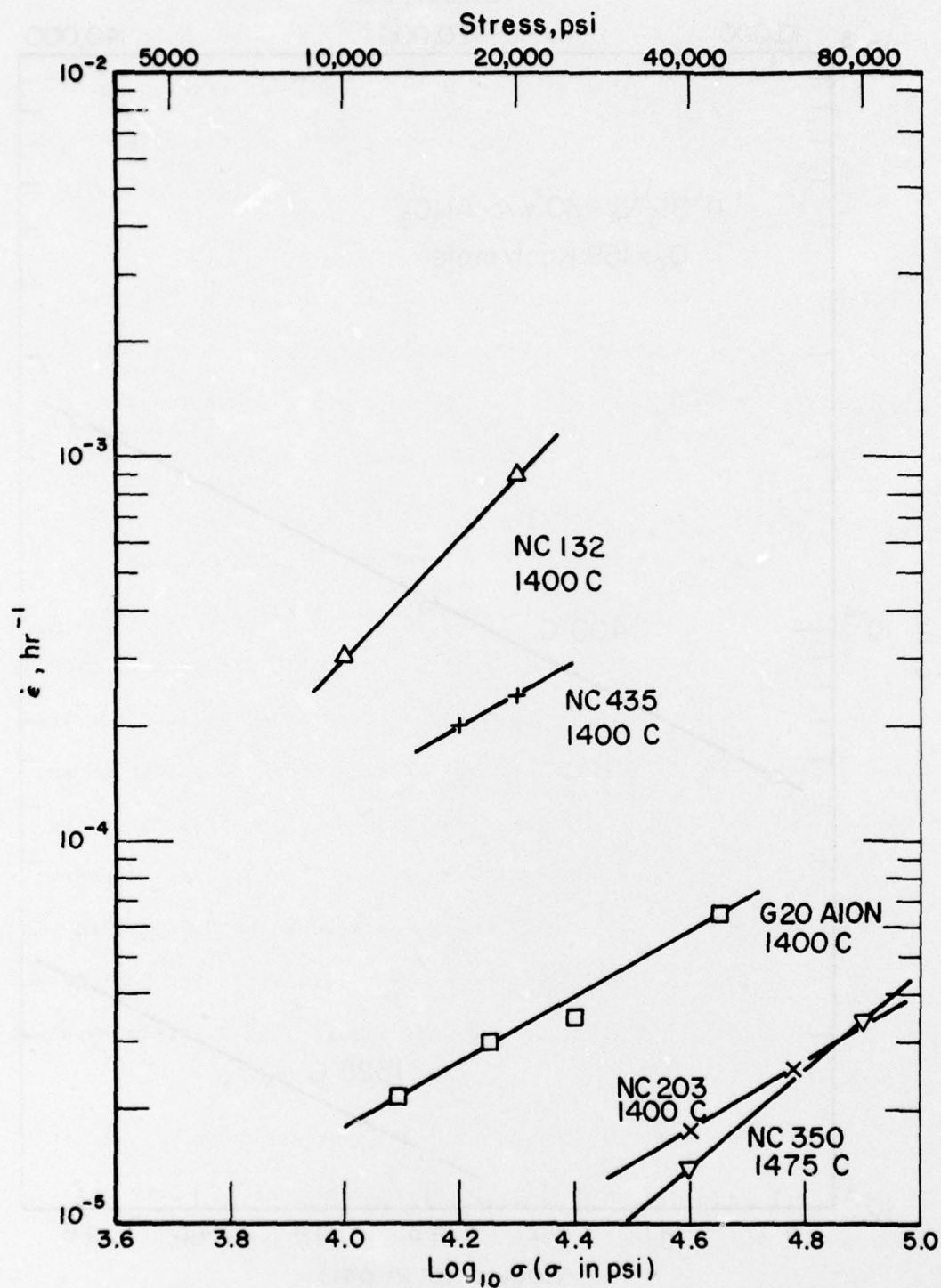


FIGURE 25. COMPARISON OF CREEP DATA OBTAINED AS A FUNCTION OF STRESS AT 1400°C AND 1475°C IN AIR FOR HOT PRESSED Si_3N_4 , REACTION BONDED Si_3N_4 AND SIALON G20ALON

to any material tested in this program. At 1400°C under a stress of 50,000 psi the creep rate in air was measured at $6.67 \times 10^{-6} \text{ hr}^{-1}$, which is the lower limit of detectability for a 370-hr. test. Subsequent testing was performed at 1475°C in order to obtain measurable strains in reasonable time periods. Results obtained at 1475°C are included in Figure 25 and were two orders of magnitude lower than those obtained at 1400°C for NC132, the best hot-pressed silicon nitride material available. The creep strength for NC350 was also superior to the best SiAlON tested in this program. The stress exponent n for NC350 at 1475°C was found to have a value of 1.3, based on two creep rates, obtained at the lower limit for which accurate measurements could be made.

The limited creep data obtained for the two silicon carbide materials tested in this program suggest that the hot-pressed NC203 has outstanding compressive creep resistance, while the NC435, although apparently superior to NC132, has severe deficiencies. The hot-pressed silicon carbide yielded creep rates at 1400°C some two orders of magnitude lower than those measured for hot-pressed silicon nitride, requiring applied stresses on the order of 40,000 psi to get creep rates of $2 \times 10^{-5} \text{ hr}^{-1}$. The stress exponent from the limited data shown in Figure 25 was calculated to be 0.88. This suggests that the operative creep mechanisms may be different for hot-pressed SiC and hot-pressed Si_3N_4 , where the latter material yielded a stress exponent at 1400°C close to 2.0.

The results shown in Figure 25 for NC435 suggest that this material has moderately adequate creep strength at 1400°C. However, the data for this composition of silicon carbide were obtained with some difficulty. At stresses above 20000 psi the specimen failed rapidly after undergoing strain on the order of 0.2-0.4 percent, by a process that appeared

to consist of shear and decohesion parallel to the stress axis. This was the only material tested in the program which failed in such a mode, and the only material in which observable cracking occurred at strains of less than one percent. The data shown in Figure 25 were generated at applied stresses of 16000 and 20000 psi, with failure occurring after 2.0 percent strain at the higher stress. The stress exponent from the meager data available suggest a stress exponent of one.

SECTION V

DISCUSSION

Based on the differences in stress dependence and apparent creep activation energies found in this and other studies, different creep mechanisms are operative for Si_3N_4 as compared with some of the SiAlON materials, and the best SiAlON may have creep strength superior to Si_3N_4 at temperatures above 1300°C . This will be true, for example, if the creep of hot-pressed Si_3N_4 is controlled by the presence of magnesium silicate or some other glassy phase which promotes grain boundary sliding, particularly at higher temperatures, while the SiAlON creeps by a mechanism which is not controlled by a viscous grain boundary phase. As discussed previously the results for HS130 and NC132 which include the finding of a stress exponent of about 2 have been interpreted in terms of a grain boundary sliding mechanism, where creep rates are accelerated by increases in calcium content in a grain boundary phase.⁽¹²⁾ In this analysis the experimental stress dependence is said to result from a change in the effective area supporting the applied load as wedge cracks nucleate and grow. Thus we have the expected linear stress dependence of a viscous flow process modified by a change in the effective stress by void formation.

Support for the hypothesis that grain boundary sliding is the dominant mode for deformation of hot-pressed Si_3N_4 was obtained from several crept NC132 samples, examined by transmission electron microscopy by Drs. B. G. Pletka and H. H. Heuer at the Case-Western Reserve University. Results obtained from a tension creep specimen NC132-T4 which was deformed at 1325°C under 5000 psi in a vacuum of 10^{-5} torr to total strain of 1.1% are shown in Figures 26 and 27. Specimens had been prepared by ion thinning

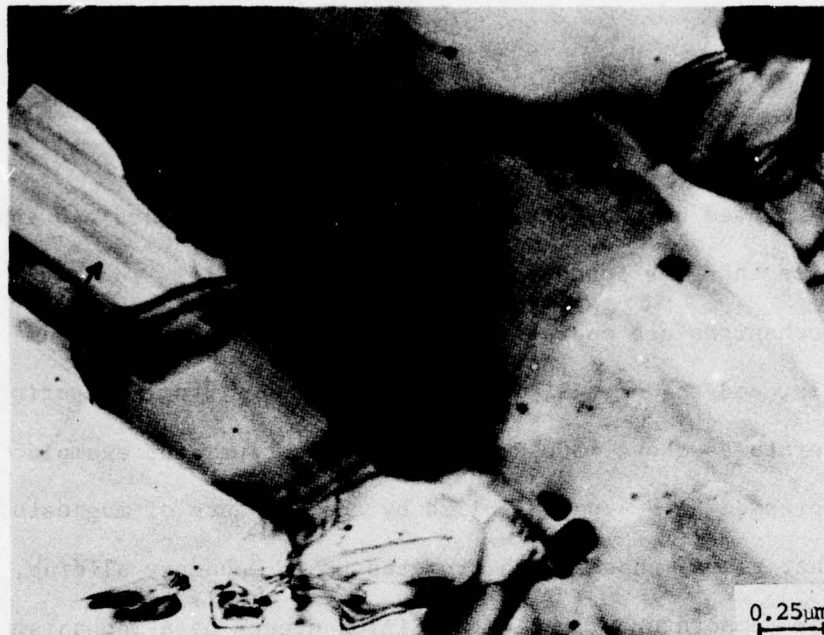


FIGURE 26. FOIL OF NC-132-T4 ILLUSTRATING OPAQUE PARTICLES, DISLOCATION ARRAYS WITHIN GRAINS, AND APPARENT STACKING FAULT CONTRAST (ARROWED).

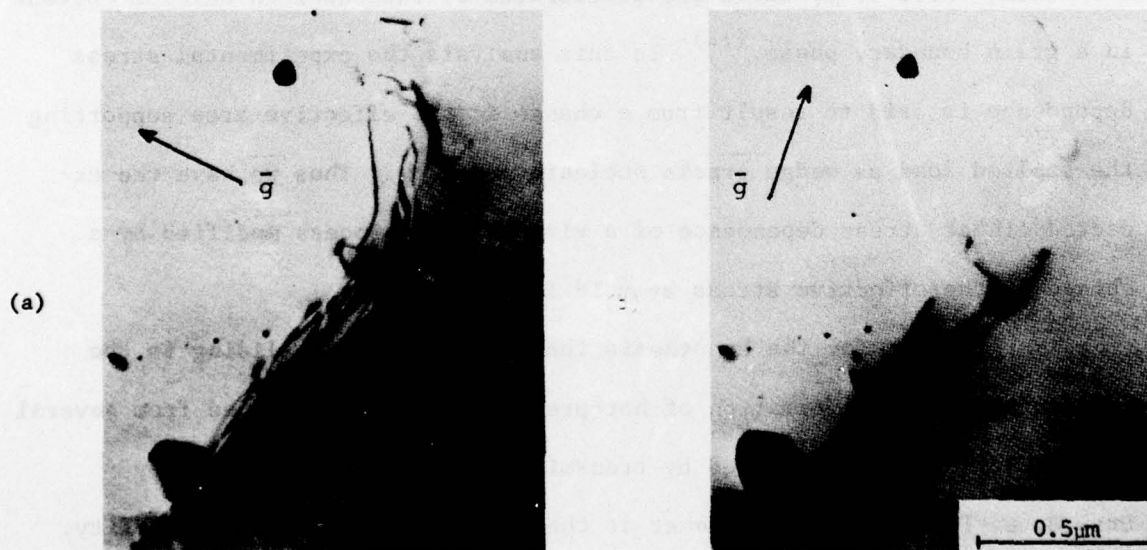


FIGURE 27a. DISLOCATIONS IN AN α GRAIN OF NC-132-T4; $\vec{g} = [0004]$.

FIGURE 27b. SAME AREAS AS FIGURE 27a SHOWING ONE SET OF DISLOCATIONS OUT OF CONTRAST FOR $\vec{g} = [6060]$. These dislocations have $\vec{b} = \langle 0001 \rangle$. After Pletka.

of slabs cut at 45° to the tension axis which had been mechanically ground to $\sim 50 \mu\text{m}$.

The Case-Western Reserve University workers have observed the electron opaque particles shown in Figures 26 and 27 in all foils examined to date. The particles appear to be present in nearly every grain. These particles, up to $0.2 \mu\text{m}$ in diameter are believed to be tungsten carbide contaminant, although positive identification has not yet been made. Examples of the dislocation arrays observed are included in Figure 27. The Burgers vector of the dislocations visible in Figure 27(a) has been identified as $\langle 0001 \rangle$.

Grain boundary triple points have been observed, particularly in the highly strained compression creep specimens, suggesting, in accord with previous results, that grain boundary sliding makes a major contribution to the total observed deformation. This theory has been proposed by Kossowsky⁽²²⁾, and more recently by Ud Din and Nicholson⁽¹³⁾ who also presented electron microscopic evidence to suggest that creep behavior of hot-pressed Si_3N_4 could be ascribed to grain boundary sliding accommodated by void formation of triple points and by limited local plastic deformation.

Diffusional activation energies for silicon and nitrogen in Si_3N_4 are unknown, so it is not possible to adequately discuss all the possible interpretations of the creep activation energies. Kossowsky suggests that the activation energy for creep of HS130 is comparable to that for the activation of viscous flow of silicate glasses, lending credence to his view that creep behavior of hot-pressed Si_3N_4 is governed by the viscous flow of the grain boundary glass phase. The similarity of stress dependencies and activation energies obtained in both compression and tension creep experiments indicates that the same mechanism is operative for both modes of creep over the entire range of experimental conditions.

The creep mechanism operative for SiAlON materials with low Al_2O_3 concentration, however, does not appear to be the same one controlling deformation in silicon nitride. The linear stress dependence and substantially lower creep activation energy measured for the SiAlON points to the operation of a bulk or grain boundary diffusion controlled process such as Nabarro-Herring or Coble creep. In this case the creep activation energy can be expected to be comparable to a bulk or grain boundary diffusion energy for silicon or nitrogen. The precise nature of the rate controlling species cannot be determined until diffusion data are available.

As a result of the difference in stress dependencies and activation energies for some SiAlON materials and Si_3N_4 , relative creep strengths are expected to vary with temperature and stress. At high temperatures and high applied stresses, the SiAlON materials clearly have superior creep strength; whereas the hot-pressed Si_3N_4 provides better properties at lower temperatures (below about 1250°C) and stresses. This latter behavior may result from a more rapid bulk diffusion in the expanded hexagonal SiAlON lattice than in the Si_3N_4 . Thus, if the viscous grain boundary phase can be eliminated from Si_3N_4 , the inherent strength of this material may be greater than that of SiAlON.

A crossover in creep strengths occurs (Figure 15) at about 1300°C under 10000 psi for NC132, the best hot-pressed Si_3N_4 , and specimen 59D, a moderately porous SiAlON. As shown in Figure 19, however, even the most porous SiAlON materials have greater creep strength than HS130 at 1400°C , at stresses as low as 2000 psi. There is obviously considerable uncertainty regarding the absolute values for the creep strengths which may be ultimately obtained in SiAlON and hot-pressed Si_3N_4 , but results

to date suggest that SiALON offers greater potential for high temperature, high stress applications. It must be noted that these conclusions are based on compression creep results. Different results may obtain if experiments are performed on bend specimens where slow crack growth is an important factor in establishing high temperature potential.

A comparison of the optical micrographs in Figure 1 with the experimental results included in Figure 17 shows that the creep strength of SiALON is directly dependent on material density; creep rates decreasing by an order of magnitude as the density increases from 2.71 g/cm^3 to 3.15 g/cm^3 . Since the best SiALON tested to date, G20ALON, was not a fully dense material, further increases in strength can be expected simply on the basis of density considerations. However, changes in chemistry may also influence creep strength of these materials. Thus other considerations, including grain size, alloying additions, and impurity control may offer additional means for improving the creep strength of both Si_3N_4 and the SiALON materials.

The SiALON materials prepared at Westinghouse and containing more than 40 w/o Al_2O_3 exhibited creep properties similar to those for hot-pressed Si_3N_4 and different from all other SiALON compositions employed in this study. The high stress exponent and creep activation energy found for the 40-50 w/o Al_2O_3 -containing SiALON compositions are evidence that the grain boundary sliding mechanism which controls the creep behavior of hot-pressed silicon nitride is operative for these materials as well. The fact that the same high activation energy obtained for material which exhibited linear and power law stress dependencies suggests that the same diffusion mechanism controls both creep processes in the Westinghouse SiALON compositions.

Results obtained to date suggest that only minimal variations in creep strength can be expected from changes in stoichiometry of silicon

nitride. The detailed nature of the atomic point defect structure of Si_3N_4 and related compounds, is unknown. Wild et al.⁽²³⁾ have hypothesized that the α -phase is really an oxynitride with a range of homogeneity. They suggested that the α and β phases are not merely low and high temperature forms as previously supposed but are, respectively, "high oxygen potential" and "low oxygen potential" modifications. If true, then variations in environment, e.g., nitrogen and oxygen partial pressure, might have been expected to produce effects similar to those found for creep of oxides and sulfides where orders of magnitude variation in creep rates were observed as the concentrations of native vacancies and interstitials were varied through the control of the cation/anion ratio. In view of our limited understanding of the point defect structure of Si_3N_4 conclusive statements regarding stoichiometry effects cannot be made at this time.

As shown in Figures 13 and 20, creep rates for Si_3N_4 and SiAlON obtained in air, argon, nitrogen and vacuum vary by no more than a half-order of magnitude at 1400°C. The somewhat higher creep rates obtained from specimens tested in air may be attributed to the effects of surface oxidation rather than to changes in bulk Si/N ratio which thereby control the point defect disorder of the materials tested. For example, Kossowsky suggests that the higher creep rates obtained in air result from an increase in the volume of glass formed by solution of oxidation products at the surface. Diffusion processes in silicon nitride are possibly too slow at 1400°C to produce detectable stoichiometry changes in several hundred hours. A conclusive test of the lack of influence of N_2 on creep strength would require equilibration under various nitrogen pressures at temperatures approaching the melting point, followed by creep tests at comparable or lower temperatures.

Figure 15 shows that tensile creep rates for NC132 are higher than those measured in compression. Kossowsky et al.⁽¹²⁾ suggest that this is a

consequence of grain boundary sliding involving rigid nondeformable grains. Alternatively, the higher creep rates measured in tension may result from the presence of surface flaws which increase the effective stress on the specimens.

The results included in Figure 21 suggest a small orientation dependence for the creep behavior of SiAlON 65C which appears to have a nearly equiaxed grain structure (see Figure 3(d)). Major improvements in creep strength of silicon nitride and SiAlON might be achieved by proper processing techniques. For example, the structure of HS130 presented in Figure 4(b) consists of elongated grains along with smaller equiaxed grains. If, during hot pressing, an aligned elongated grain structure could be obtained to produce a high grain aspect ratio (i.e., the ratio of grain length, L , to grain width, l), substantial improvements could be anticipated in high temperature strength, where grain boundary sliding is an important mode of deformation.

According to Wilcox and Clauer⁽²⁴⁾ the influence of grain aspect ratio (GAR) on high temperature strength can be formulated as follows: The creep or yield strength is given by:

$$\sigma = \sigma_e + K \left(\frac{L}{l} - 1 \right) \quad (1)$$

where σ_e is the strength for $L/l = 1$ (equiaxed grains) and K is defined as the GAR coefficient. For nickel - 20w/oCr - 2v/oThO₂ alloys, creep strength has been enhanced by a factor of 20 through proper thermomechanical processing to develop high grain aspect ratios.

SECTION VI

CONCLUSIONS

1. High-temperature tensile and compressive creep of hot-pressed silicon nitride is characterized by an activation energy of 168 ± 5 kcal/mole and a power-law stress dependence with $1.8 < n < 2$.
2. At 1400°C, test atmosphere has a minimal influence on creep behavior; creep rates are a factor of five greater for tests conducted in air as compared with those performed under argon, and nitrogen has intermediate effect.
3. Compression creep behavior of SiAlON materials containing small concentrations of x-phase are characterized by an activation energy of 94 kcal/mole and a linear stress exponent.
4. The creep activation energy for SiAlON materials containing high x-phase concentrations is 152 ± 9 kcal/mole while the stress exponent is about 1.75.
5. Creep rates for the SiAlON materials tested in this study increased with decreasing density, but even the lowest density materials tested (2.71g/cm^3) had greater creep strength at 1400°C than hot-pressed silicon nitride.
6. For the SiAlON materials tested in this study, creep strength generally increased with decreasing Al_2O_3 concentration.
7. Reaction-bonded silicon nitride (NC350) has the greatest compressive creep strength of all the silicon-base materials tested, including hot-pressed silicon carbide (NC203), which is, in turn, superior to hot-pressed silicon nitride at 1400°C.

8. Different creep mechanisms have been found to be operative for some SiAlON materials, as compared with hot-pressed silicon nitride. While the creep behavior of silicon nitride could be ascribed to grain boundary sliding accommodated by void formation, the predominate mode for creep of most SiAlON materials appears to involve viscous creep controlled by self-diffusion.

REFERENCES

1. P. K. Talty and M. S. Seltzer, "High Temperature Compressive Creep of Yttria Stabilized Zirconia," ARL-TR-75-0023, March 1975.
2. M. S. Seltzer and P. K. Talty, J. Amer. Ceram. Soc., 58, 124 (1975).
(Also see: M. S. Seltzer and P. K. Talty, "Creep of Low Density Yttria/Rare Earth Stabilized Zirconia" in Deformation of Ceramic Materials, R. C. Bradt, Ed., Plenum Press, 1975, p. 297.)
3. N. L. Parr, G. F. Martin, and E.R.W. May in Special Ceramics, ed. P. Popper, Haywood and Col., London, 1960, p. 102.
4. G. G. Deeley, J. M. Herbert, and N. C. Moore, Powder Metallurgy, 8, 145 (1961).
5. F. F. Lange and G. R. Terwilliger, "Fabrication and Properties of Silicon Compounds," Final Report on Contract N00019-71-C-0107, NASC, January, 1972.
6. D. E. Lloyd, Special Ceramics 4, P. Popper, Ed., British Ceramic Research Assoc., Stoke-on-Trent, 1968, p. 165.
7. A. G. Evans and J. V. Sharp, J. Materials Science, 6, 1292 (1971).
8. D. S. Thompson and P. L. Pratt, Proc. Brit. Ceramic Soc., 6, 37 (1966).
9. N. L. Parr, R. Sands, P. L. Pratt, E.R.W. May, C. R. Shakespeare, and D. S. Thompson, Powder Metallurgy, 8, 152 (1961).
10. E. Glenny and T. A. Taylor, Powder Metallurgy, 8, 164 (1961).
11. N. L. Parr, Research, 13, 261 (1960).
12. R. Kossowsky, D. G. Miller, and E. S. Diaz, "Tensile and Creep Strengths of Hot-Pressed Si_3N_4 ," Westinghouse Research Laboratories, Scientific Paper 74-904-FORAM-P8, August, 1974.
13. S. Ud Din and P. S. Nicholson, J. Materials Science, 10, 1375 (1975).
14. S. Ud Din and P. S. Nicholson, J. Amer. Ceram. Soc., 58 500 (1975).
15. J. A. Mangels and D. F. Watt, Bull. Amer. Ceram. Soc., 53, 395 (1974).
16. W. J. Arrol, "The SiAlONs-Properties and Fabrication," presented at the Army Materials Technology Conference on Ceramics for High Performance Applications, Hyannis, Mass., Nov. 19, 1973.
17. T. R. Wright and D. E. Niesz, "Improved Toughness of Refractory Compounds," NASA CR-134690, October, 1974.
18. F. F. Lange, "Fabrication and Properties of Silicon Compounds," Final Report, Contract N00019-73-C-0208, NASC, Feb. 26, 1974.

19. M. E. Washburn and H. R. Baumgartner, "High Temperature Properties of Reaction Bonded Silicon Nitride" in Ceramics for High Performance Applications, J. J. Burke et al., eds. Brook Hill, 1974, p. 479.
20. E. W. Hauck, Gas Turbine World, Sept. 1974, p. 17.
21. A. H. Clauer and B. A. Wilcox, "High Temperature Tensile Creep of Magnesium Oxide Single Crystals," submitted to Phil. Mag.
22. R. Kossowsky, J. Materials Science, 8, 1803 (1973).
23. S. Wild, P. Grieveson, and J. H. Jack, "The Crystal Structure of Alpha and Beta Silicon and Germanium Nitrides," Special Ceramics 5, Brit. Ceram. Res. Assoc. Stoke-on-Trent, 1973.
24. B. A. Wilcox and A. H. Clauer, "Dispersion Strengthening in the Super-alloys," C. T. Sims and W. C. Hagel, Eds., Wiley, New York, 1972, p. 197.